He atom in a quantum dot: Structural, entanglement, and information-theoretical measures

Santanu Mondal [1], Kalidas Sen [2,*] and Jayanta K. Saha [1,†]
[1]*Department of Physics, Aliah University, IIA/27, Newtown, Kolkata 700160, India*
[2]*School of Chemistry, University of Hyderabad, Hyderabad 500046, India*

(Received 14 November 2021; accepted 17 March 2022; published 29 March 2022)

Energy eigenvalues of ground and singly excited $1sns$ ($^{1,3}S$) ($n = 2 - 5$, being the principal quantum number) states of a He atom in a quantum dot have been investigated in detail by incorporating explicitly correlated Hylleraas-type wave functions in the framework of the Ritz variational method. The quantum dot environment is simulated by considering the influence of the finite oscillator (FO) potential. We have examined the behavior of different energy components contributing to the total energy. In this regard, the Hund's spin multiplicity rule for $1sns$ ($^{1,3}S$) ($n = 2 - 5$) states of a He atom has been examined in depth in terms of observed unusual ordering of the electron repulsion and total energy. The energy contribution due to the total correlation (in the presence of both radial and angular correlation) effect, the radial correlation limit and angular correlation limit of a He atom under different strengths of the FO potential have been studied. As a quantitative replication of our results, we have introduced and verified the Hellmann-Feynman theorem and virial theorem for both a He atom and its first ionization threshold, i.e., He^+ ($1s$, ^2S) ion under the influence of the FO potential. The expectation value of different radial quantities r_1, r_1^2, r_{12}, r_{12}^2, $r_< = \min(r_1, r_2)$, $r_> = \max(r_1, r_2)$, angular quantities, e.g., interparticle angles θ_1, θ_{12}, one-electron delta function $\delta(\vec{r}_1)$, and two-electron delta function $\delta(\vec{r}_{12})$ have been determined for different strengths of the FO potential. The effect of the FO potential on the quantum similarity index and dissimilarity between the He^+ ($1s$, ^2S) and He ($1s^2$, ^1S and $1s2s$, $^{1,3}S$) as well as between He ($1s2s$, ^1S) and He ($1s2s$, ^3S) has been examined. The von Neumann, linear, and Shannon information entropy for the ground state He atom have been computed to ascertain the characteristic features of the electronic entanglement and the charge distribution under the FO potential.

DOI: 10.1103/PhysRevA.105.032821

I. INTRODUCTION

Fabrication of quantum systems with increasingly precise control has been identified [1] as the main research activity in atomic, molecular, and optical science and technology in the coming decade. In this context, the breakthrough advances in the design and fabrication of nanoscale electronic devices depend on our understanding of the structure and stability of quantum confined electronic systems. Theoretical studies in this direction have considered different types of phenomenological potentials to model atoms or ions within different confining environments [2–15]. The theoretical investigation on quantum dots (QDs) has attracted special attention due to its wide range of applications in biotechnology, modeling molecules with tunable bonds, semiconductors, LEDs, transistors, diode lasers, solar cells, and medical imaging [16–22]. The electronic and optical properties of the QDs or artificial atoms are very similar to the normal atoms.

Different types of electronic and optical properties for such low-dimensional QDs have been investigated by considering various types of model potentials like Coulomb, harmonic, rectangular, parabolic, finite oscillator (FO), Woods-Saxon, Poschl-Teller, Rosen-Morese, Tietz, and Eckart potential [23–38] to mimic the modified interactions. Among these, one of the most preferred model potentials is the FO potential, which has flexibility in changing its shape and size by tuning the depth and width of the potential. Winkler [29] used the FO potential to analyze the effect of such potential on the bound and resonance state of a He atom using a complex coordinate rotation method and excluding the electron-electron correlation effect. However, the uncertainties in his calculation could not be removed even after the explicit inclusion of the correlation effect. Later, Kimani *et al.* [31] used this FO potential to study the ground states of few-electron QDs through a restricted Hartree-Fock (RHF) method by including the electron correlation effect, stepwise, in a series of approximations based on the single particle Green's function approach. Chakraborty and Ho [32] investigated the effect of FO potential on the resonance state of two electron atoms in the framework of the stabilization method by including the electron correlation effect and expanding the wave function in a single exponent Hyllaraas-type basis. The position of the bound states and the parameters of resonance states of He atoms have been investigated by Saha *et al.* [30] and Jiao and Ho [39] by considering correlated basis sets. Ou *et al.* [19] used both attractive and repulsive FO potentials to estimate the energy eigenvalue corresponding to the ground state and singly excited state of He atoms. It is evident that most of the work reported in the literature is focused mainly on the variation of the energy eigenvalue of a few low-lying

*kalidas.sen@gmail.com
†jksaha.phys@aliah.ac.in

 ©2022 American Physical Society

bound and resonance states of He atoms trapped inside a QD environment.

Our aim in the present paper is to study the detailed variation of a *comprehensive* set of the structural properties of a He atom by tuning the parameters (depth V_0 and width Δ) of the confining FO potential simulating a QD environment. The same system can alternatively be treated as a two-electron QD with an attractive Coulomb impurity at the center. A minimalistic extension of the present method can also throw light on the properties of two-electron QDs with repulsive Coulomb impurity at the center. The results presented in this paper are meant to accurately characterize the model system under consideration. For this purpose, we have adopted Ritz variational framework where the wave function is expanded in an explicitly correlated multiexponent Hylleraas-type basis set. In the present case, the cavity width Δ has been changed in a wide region between 0.001 a.u. to 1000 a.u. while the cavity depth V_0 has been set with values 0.2 a.u., 0.5 a.u., and 1.0 a.u. Different important geometrical properties of the ground state and a few singly excited states of He atoms have been estimated and we have found that there is a considerable change in all geometrical properties within the approximate range $0.1 - 10.0$ a.u. of the cavity width for any constant value of cavity depth V_0. For free He atoms, there are several works [40–42], but to the best of our knowledge, there exist no similar estimations for He atoms under such a confining environment (mimicked by FO potential). It has also been noted that the variation of different energy components of the same states of a He atom has a sharp change within the same region of cavity width Δ and for any value of cavity depth V_0. An interesting part in the study of energy components in this paper relates to the study of the validity of Hund's rule for the singlet and triplet states arising from He in $1sns$ ($n = 2 - 5$) configuration in conjunction with the relative ordering of the electron repulsion energy. The linear dependency of the total energy on the potential energy components and kinetic energy of the confined He atom as well as a He^+ ion have been derived by applying the suitable version of the Hellmann-Feynman and the virial theorems. We have observed that the energy components obtained from Hellmann-Feynman and virial theorems are very much consistent with the results estimated from the present correlated variational approach. A study of the variation of the electron correlation energy for the ground-state He atom has been done. This has been achieved via the accurate B-spline basis calculations of the Hartree-Fock energy (E_{HF}) for the ground state of the confined He atom. The correlation energy is estimated using Lowdin's definition as $E_{\mathrm{corr}} = E_{\mathrm{exact}} - E_{\mathrm{HF}}$. Further, we have analyzed the radial and angular correlation limit of the correlation energy for different cavity parameters. It is to be mentioned that in contrast to the angular correlation, the energy contribution from the radial correlation has a distinct peak within the approximate range 0.1–10.0 a.u of cavity width Δ. The quantum similarity index (QSI)between two different one-electron densities has been estimated to quantify the similarity or the lack of it among the various spin states arising from the different electronic configurations of the confined He atom. The changes in quantum similarity and dissimilarity index among He^+ ($1s$, ^2S), He ($1s^2$, ^1S), He ($1s2s$, ^1S), and He ($1s2s$, ^3S) has also been analyzed in detail by tuning cavity parameters. In this context, our estimated result clearly reflects the fact that the similarity or dissimilarity between two quantum states can be manipulated by solely tuning the cavity parameters.

Another intriguing phenomenon in quantum mechanics is the quantum entanglement which has no classical analog. Recently, the study of quantum entanglement has become a subject of great interest among researchers, as such study plays an important role in different research areas like quantum information, quantum teleportation, quantum computation, and quantum cryptography [43–46]. One of the most important aspects of the entanglement measures is that it can be used as an alternative way to quantify the quantum correlation. Interestingly, it is now possible that by controlling the nanostructure parameter in a nanodevice, the amount of entanglement of an atom or ion in a QD can be manipulated. Researchers have already made several efforts to study the quantum entanglement corresponding to the bound and resonant states of free He atoms and He-like ions [47–59]. Besides, few investigations on the entanglement measurement of He atom under Debye palsmas are also present in literature [60,61]. An interesting piece of work related to the estimation of quantum entanglement for two interacting ultracold bosonic atoms in one-dimensional harmonic traps is by Peng and Ho [62]. However, there are very few works on the measure of the quantum entanglement corresponding to He-like atoms or ions under QDs [63–71]. For instance, Coden *et al.* [69] studied the effects of Coulomb impurities on the entanglement and investigated all the possibilities of manipulating the entanglement of the electrons through completely controlling the parameters of the Gaussian attractive potentials, while Kóscik [70] estimated the von Neumann entropy corresponding to different S states of two Coulombically attracting electrons by considering the harmonic potential in the presence of a off-center Coulomb impurities. Kóscik and Saha [71] analyzed the effect of the FO potential on the ground state of He atoms by considering the trial variational wave function expanded in a perimetric Hylleraas-type basis set. A nonmonotonic behavior of the von Neumann entropy and the linear entropy of the ground state of the He atom under the confining FO potential has been noted and it is worth mentioning that these entropies can easily be manipulated through tuning the cavity parameters. In the present paper, we have reproduced and verified the results obtained by Kóscik and Saha [71]. In addition, we have investigated the variation of linear entropy for different parameters of the FO potential.

Recent years have witnessed an overwhelming interest among researchers in different branches of physics and chemistry about the theoretical estimation of quantum information entropy [72–76]. The characterization of the atomic and molecular systems in terms of the information theoretical measures, such as the Shannon entropy and the Fisher information at the classical level and the von Neumann and other entanglement measures [77,78] at the quantum level, complements their quantum mechanical description based mostly on the total electronic energy. The information theoretical analysis is generally carried out in terms of the entropic spreading measures of the electron distribution using the one-electron and two-electron pair densities [75,79–87] as the key parameters. The various measures are then used to quantify the uncertainty, randomness, disorder, localization, and

electron correlation effects of N-electron systems. While the one-electron density has been extensively used in the analysis, there have been several recent studies which involve the information theoretical measures using the electron pair densities. In this paper, we report the results of our calculations, Shannon information entropy using the one-electron density, $\rho(r)$ and the linear entropy S_L, and von Neumann entropy S_{vN} in terms of reduced density matrix, ρ_{red}, from the Hylleraas wave functions. We note here that the entanglement entropic study undertaken here explicitly includes the spatial electron correlation effects which specifically define the nature of chemical binding in the He atom confined inside the finite HO potential. Further, the accurate numerical results reported here will be useful in precisely defining the present system and differentiating it from those containing the He atom embedded inside the various other confining potentials. A detailed information theoretical study including the relative information entropy derived from the Hartree-Fock and correlated pair densities for the present system is currently under progress and will be published separately. Extensive calculations of the quantum information entropy have been reported for free and confined hydrogen, He, and He-like atoms [19,28,74–76,88–90]. Sen [91] made a detailed study on Shannon entropy for both hydrogenlike and He-like ions by considering infinite confinement. Ou *et al.* [19] investigated the Shannon information entropy in position space corresponding to the ground and singly excited states of He atoms by considering attractive as well as repulsive FO potentials and correlated Hylleraas wave functions were used to estimate the Shannon entropy. In the present paper, we have made a detailed investigation on the variation of the Shannon information entropy corresponding to the ground state of a He atom and the result shows reasonable agreement with Ref. [19]. It is found that the influence of the confining potential determines the entropy of the system and thereby shows the variations of the electron localization. We have organized our paper as follows: the present methodology has been discussed in Sec. II. The results obtained in the paper have been presented and discussed in detail in Sec. III. A summary of the main conclusions obtained in this paper is presented in Sec. IV.

II. METHOD

A. Hamiltonian

The nonrelativistic Hamiltonian describing a two-electron system (atomic unit is used throughout unless otherwise specified) inside a cavity is given by

$$\mathcal{H} = -\tfrac{1}{2}\nabla_1^2 - \tfrac{1}{2}\nabla_2^2 + V_{\texttt{eff}}, \tag{1}$$

where the subscripts 1 and 2 represent the electrons. The first two terms in Eq. (1) are the kinetic energy of electrons and the last term is the effective potential of the system. Here, the interparticle distance r_{12} is defined as $r_{12} = |\vec{r}_{12}| = |\vec{r}_1 - \vec{r}_2|$. The effective potential $V_{\texttt{eff}}$ of the system is given by

$$V_{\texttt{eff}} = \sum_{i=1}^{2}\left[-\frac{2}{r_i} + V_{\text{FO}}(r_i)\right] + \frac{1}{r_{12}}. \tag{2}$$

The first part within the summation of Eq. (2) is the Coulomb attractive potential between the electrons and the nucleus. The second term represents the interaction potential between the electrons and the cavity while the third part represents the Coulomb repulsive potential between the two electrons. In this present paper, the QD environment has been characterized by the spherically symmetric FO potential [31,32,71], which takes the form

$$V_{\text{FO}}(r) = -V_0(1 + c_w r)e^{-c_w r}, \tag{3}$$

where V_0, c_w are the depth of the potential well and cavity constant, respectively. The cavity constant is defined as

$$c_w = \frac{1}{\Delta\sqrt{V_0}}, \tag{4}$$

where the term Δ represents the width of the potential. By tuning the parameters V_0 and Δ, the size of the cavity potential can be changed. It is interesting to note that for a fixed value of c_w, the harmonic nature of the potential $V_{\text{FO}}(r) \sim r^2$ can be observed at the limit $r \to 0$, i.e., very near to the center of the QD, the FO potential behaves as a harmonic potential. In contrast to this, for the large value of r ($\to \infty$), the potential deviates from the harmonic nature and it becomes a quite similar profile to the Gaussian potential.

B. Correlated wave function

We constructed our trial wave function of any bound $^{1,3}S$ state of He atoms by expanding in the Hylleraas-type basis set of the type

$$\Psi(r_1, r_2, r_{12}) = (1 + \kappa\hat{P}_{12})\sum_{i=1}^{N} C_i\chi_i, \tag{5}$$

where, $\chi_i = r_1^{l_i} r_2^{m_i} r_{12}^{n_i} e^{-\alpha_i r_1 - \beta_i r_2}$ with $l_i + m_i + n_i \leqslant w_i$ and w_i, l_i, m_i, n_i are positive integer or zero. The coefficients C_i ($i = 1, 2, ..., N$; N represents the total number of terms in the wave function) in Eq. (5) are the linear-variational parameters, while the $2N$ number of exponents α_i and β_i ($i = 1, 2, ..., N$) are the nonlinear variational parameters ($\alpha_i > 0$, $\beta_i > 0$). In Eq. (5), $\hat{P}_{12}$ represents the permutation operator between the two identical electrons in the He atom. For the singlet state, the value of κ is $+1$ and $\kappa = -1$ for the triplet state. To find the optimal choice of the nonlinear parameters α_i and β_i ($i = 1, 2, ..., N$), we applied the Nelder-Mead optimization technique [92]. Further, the nonlinear parameters α_i's and β_i's in Eq. (5) are chosen quasirandomly from a two-dimensional box. Here, the simplest version of the procedure to choose the nonlinear parameters has been explained in the following way. Let the index i ($1 \leqslant i \leqslant N$) be such that p=mod$(i, 3) + 1$, where mod$(i, 3)$ represents the modular division or the integer remainder due to the division of i by 3. Therefore, the nonlinear parameters α_i and β_i can be chosen from the two positive intervals $[\mathcal{A}_1^{(p)}, \mathcal{A}_2^{(p)}]$ and $[\mathcal{B}_1^{(p)}, \mathcal{B}_2^{(p)}]$ as follows:

$$\begin{aligned}\alpha_i &= \left\langle\left\langle \tfrac{1}{2}i(i+1)\sqrt{2}\right\rangle\right\rangle\left(\mathcal{A}_2^{(p)} - \mathcal{A}_1^{(p)}\right) + \mathcal{A}_1^{(p)},\\ \beta_i &= \left\langle\left\langle \tfrac{1}{2}i(i+1)\sqrt{3}\right\rangle\right\rangle\left(\mathcal{B}_2^{(p)} - \mathcal{B}_1^{(p)}\right) + \mathcal{B}_1^{(p)},\end{aligned} \tag{6}$$

where the notation $\langle\langle A \rangle\rangle$ represents the fractional part of the real number A. It is to be noted that there is no restriction whether $\mathcal{A}_2^{(p)} \geqslant \mathcal{A}_1^{(p)}$ or $\mathcal{A}_1^{(p)} \geqslant \mathcal{A}_2^{(p)}$, which is also true for $\mathcal{B}_1^{(p)}$ and $\mathcal{B}_2^{(p)}$. Further, it is also true that for any value of p,

the value of the relative position of the interval $[\mathcal{A}_1^{(p)}, \mathcal{A}_2^{(p)}]$ can be arbitrary with respect to the interval $[\mathcal{A}_1^{(p+1)}, \mathcal{A}_2^{(p+1)}]$ or $[\mathcal{A}_1^{(p-1)}, \mathcal{A}_2^{(p+1)}]$. The same is also true for the interval $[\mathcal{B}_1^{(p)}, \mathcal{B}_2^{(p)}]$. Therefore, the bound-state energies are obtained by solving the generalized eigenvalue equation

$$\underline{\underline{\mathcal{H}}}\,\underline{C} = \mathcal{E}\underline{\underline{\mathcal{S}}}\,\underline{C}, \tag{7}$$

where the Hamiltonian matrix $\underline{\underline{\mathcal{H}}} = \langle\chi_i|\mathcal{H}|\chi_j\rangle$, overlap matrix $\underline{\underline{\mathcal{S}}} = \langle\chi_i|\chi_j\rangle$ and $\underline{C}$ is the column matrix which consists of the linear variational parameters.

C. Hartree-Fock calculations

The RHF calculations [93–95] reported in this paper for the ground state He atom have been carried out using the computer code originally written by Saito [96–98], which employs the B-spline basis set to express the radial wave functions. We refer the reader to Refs. [96–98] for a detailed description of the code. In the present paper, we have adapted the code so as to include the potential in Eq. (3) along with the standard effective one-electron Fock operator. In this section, we shall present the B-spline basis set parameters used in our calculations. The RHF orbital with symmetry λ can be written as

$$\psi_{n\lambda m}(r,\theta,\varphi) = r^{-1}P_{n\lambda}(r)Y_\lambda^m(\theta,\varphi), \tag{8}$$

where $P_{n\lambda}$ and $Y_\lambda^m(\theta,\varphi)$, respectively, denote the radial function and the spherical harmonics. The B splines of order K $\{B_{i,K}\}$ are piecewise polynomials of degree $K-1$ on a knot sequence in a cavity of radius R [99]. The knot sequence $\{t_i\}$ is a set of points defined on an interval $[0, R]$. $B_{i,K}(r)$ is nonzero in the interval $[t_i, t_{i+K})$. The $P_{n\lambda}(r)$ are expanded by the B-spline set defined in an interval $[0, R]$ with the boundary conditions $P_{n\lambda}(0) = 0$ and $P_{n\lambda}(R) = 0$. The $P_{n\lambda}(r)$ is expanded in terms of N-term B-spline set $\{B_{i,K}\}_{i=2,\ldots,N+1}$ as

$$P_{n\lambda}(r) = \sum_{i=1}^{N} C_{n\lambda,i}B_{i+1,K}(r). \tag{9}$$

In the present paper, we have used a 100-term B-spline basis set with $K = 9$ and $R = 40$ on an exponential-type knot sequence [100] with the initial interval $R_1 = 10^{-4}$. The total energy values calculated in this paper have an accuracy of 12 decimal digits in a.u.

D. Ionization threshold

To investigate the behavior of two-electron energy levels within a finite domain, it is essential to calculate the respective one-electron threshold within the confinement. The variational equation for the ground state of a He^+ ion within a FO potential can be written as

$$\delta\int_0^\infty \left[\frac{1}{2}\left(\frac{\partial f}{\partial r}\right)^2 + \left\{-\frac{2}{r} + V_{\rm FO}(r) - \mathcal{E}_{\rm th}\right\}f^2\right]r^2dr = 0. \tag{10}$$

The radial function $f(r)$ for the ground state of a hydrogenlike ion is expanded in the pure exponential basis set as

$$f(r) = \sum_i D_i e^{-\alpha_i r}. \tag{11}$$

In this calculation, we have taken 101 different nonlinear parameters α in a geometrical sequence $\alpha_{i+1} = \alpha_i\gamma$, γ being the geometrical ratio. The energy values $\mathcal{E}_{\rm th}$ and linear coefficients D_i's are determined by using equation similar to Eq. (7).

III. RESULTS AND DISCUSSIONS

The nonlinear parameters α_i's and β_i's in the exponent of the wave function defined in Eq. (5) are chosen quasirandomly from two different one-dimensional boxes, the lengths of which are initially set with two different guess values. Subsequently, the energies of the ground and singly excited bound states are optimized with respect to the box lengths for fixed values of N by adopting Nelder-Mead simplex algorithm [92]. This procedure has been repeated for He atoms with different confining parameters (V_0, Δ).

The convergence of the energy eigenvalues of the ground state and the singly excited states of a He atom with respect to the number of terms N defined in the wave function Eq. (5) has been tested for different values of the confining parameters. We have noted a consistent convergence pattern (at least up to the tenth decimal place)with respect to the enlargement of ω up to 16 ($N = 525$).

To demonstrate the accuracy of the present method, a comparison analysis of energy eigenvalues of $1s^2$ (^1S) and $1s2s$ (^1S) state of He atom with the available theoretical estimates has been made in Table I. It is clear that our estimated results show good agreement with those of Refs. [19,39,101]. For instance, Ou *et al.* [19] estimated the ground-state energy for free He atoms as -2.903724371 a.u. by considering Hylleraas-type wave functions while our estimated energy value of the same is -2.9037243768 a.u. Jiao *et al.* [39] also evaluated the energy of the same as -2.90364 a.u. with configuration interaction (CI) basis (538 terms in the wave function) and -2.90372 a.u. with Hylleraas-type basis (525 terms in the wave function) in the framework of the Ritz-variational method. One of the highly precise estimates of the nonrelativistic energy of the same state is due to Drake *et al.* [101] as -2.903724377034119479 a.u. by considering the double basis set method in Hylleraas coordinates. The same analysis has also been made for the $1s2s$ (^1S) state of a He atom. Our estimated energy corresponding to the $1s2s$ (^1S) state of a He atom with $V_0 = 1.0$ a.u. and $\Delta = 100.0$ a.u. is -3.1444769986 a.u. while the available energy of the same is given by Ou *et al.* [19] as -3.144476898 a.u. Thus, we may opine that the accuracy of our obtained results for any state and any arbitrary set of (V_0, Δ) is at least up to the order of 10^{-8} a.u.

A. Variation of energy components

The total energy eigenvalue corresponding to the ground state of He atom has been listed in Table II for different sets of (V_0, Δ). The ground-state energy of a free He

TABLE I. Comparison of present energy eigenvalues $-E$ of ($1s^2$, ^1S) and ($1s2s$, ^1S) states of He with available theoretical estimates for different cavity widths Δ and cavity depths V_0. All entities are in a.u. *a*: Drake *et al.* [101]; *b*: Jiao *et al.* (with CI-type basis) [39]; $b^\dagger$: Jiao *et al.* (with Hylleraas basis) [39]; *c*: Ou *et al.* (with Hylleraas basis) [19].

		$1s^2$, ^1S		$1s2s$, ^1S	
V_0	Δ	Present	Others	Present	Others
0.0	–	2.9037243768	2.9037243770[a]	2.1459740450	2.1459740460[a]
			2.90364[b]		2.14596[b]
			2.90372[b†]		2.14597[b†]
			2.903724371[c]		2.145974012[c]
0.2	0.01	2.9037304704	2.903730428[c]	2.1459784505	2.145978326[c]
	1.0	3.0933446236	3.093344574[c]	2.2606931719	2.260693038[c]
	100	3.3036079245	3.303607882[c]	2.5445287982	2.544528698[c]
0.5	0.1	2.9300410394	2.92997[b]	2.1646145256	2.16460[b]
			2.93004[b†]		2.16461[b†]
			2.930040819[c]		2.164613565[c]
	1.0	3.5649046788	3.56482[b]	2.5371478848	2.53713[b]
			3.56490[b†]		2.53715[b†]
			3.564904622[c]		2.537147708[c]
	100	3.9036068759	3.90353[b]	3.1444769986	3.14446[b]
			3.90361[b†]		3.14448[b†]
			3.903606833[c]		3.144476898[c]

atom is estimated as -2.90372438 a.u. while it becomes -2.90372444 a.u. for $(V_0, \Delta) = (0.5, 0.001)$ a.u. and it saturates at -3.90372318 a.u. for $(V_0, \Delta) = (0.5, 1000.0)$ a.u. However, this decrement in energy with respect to Δ for constant V_0 is not monotonic. In contrast, for constant Δ, the increment of V_0 monotonically decreases the bound-state energy. The variation of the total energy for the ground and singly excited $1sns$ ($^{1,3}S$) ($n = 2 - 5$) states of He atom with respect to Δ is depicted in Fig. 1. It is interesting to note that the ground and singly excited $1sns$ ($^{1,3}S$) ($n = 2 - 5$) energy levels of a He atom cannot overcome the He^+ ($1s$, ^2S) threshold (black dashed line) and therefore implies that it is not possible to ionize the He atom solely by tuning the parameters (V_0, Δ) of the FO potential. In Table II, we have listed different energy components, i.e., total kinetic energy E_k, Coulomb attraction energy E_a, Coulomb repulsion energy E_r, and confining FO potential energy E_c corresponding to the ground state of He atom. The cavity depth V_0 is fixed at 0.5 a.u. We notice a sharp change in the energy components E_k, E_a, and E_r for Δ ranging from 0.1 a.u to 10.0 a.u. The kinetic energy E_k is estimated as 2.90372456 a.u. for $\Delta = 0.001$ a.u. which increases 11.78% to 3.24584969 a.u. as Δ changes to 1.0 a.u. and finally attains 2.90372675 a.u. as Δ becomes 1000.0 a.u. In Figs. 2(a), 2(c) and 2(d), the respective variations of E_k, E_a, and E_r with respect to Δ are shown. It can be seen that at around $\Delta = 1.0$ a.u., E_k of ground state of He atom has a maximum. But for excited $1sns$ ($^{1,3}S$) ($n = 3 - 5$) states of He atoms, there are two distinct points of maximum of E_k. Unlike this, E_a has a single point of minima around $\Delta = 1.0$ a.u. for the ground state of He atom and there are two minimum points of E_a for the excited states $1sns$ ($^{1,3}S$) ($n = 3 - 5$) of the He atom. In case of E_r, it has a single maxima for ground and excited states of He atoms. It is worth noting that the point of maxima is shifted toward the higher Δ value as we go from the lower to upper excited state. The asymptotic behavior of the confining FO potential E_c energy can clearly be visualized from Table II. At low values of Δ ($= 0.001$ a.u.), the energy due to the confining potential is almost zero ($E_c = -0.00000006$ a.u.) and for high Δ ($= 1000.0$ a.u.) gives $E_c = -0.99999881$ a.u. ($\sim -2V_0$) with V_0=0.5 a.u. To get a more general view about such behavior of the FO potential, we have investigated the

TABLE II. Total energy eigenvalue $-E$, kinetic energy E_k, Coulomb attractive potential energy $-E_a$, Coulomb repulsive potential energy E_r, and potential energy contribution from confining finite oscillator potential $-E_c$ corresponding to ground state of He for different cavity widths Δ and cavity depths V_0. All entities are in a.u.

V_0	Δ	$-E$	E_k	$-E_a$	E_r	$-E_c$
0.0	–	2.90372438	2.90372437	6.75326720	0.94581844	0.0
0.5	0.001	2.90372444	2.90372456	6.75326741	0.94581847	0.00000006
	1.0	3.56490468	3.24584969	7.15945133	1.02286458	0.67416762
	1000.0	3.90372318	2.90372675	6.75327024	0.94581911	0.99999881
1.0	0.001	2.90372473	2.90372544	6.75326839	0.94581857	0.00000036
	1.0	4.46334161	3.41199876	7.34671803	1.06067672	1.58929907
	1000.0	4.90372318	2.90372675	6.75327025	0.94581911	1.99999880

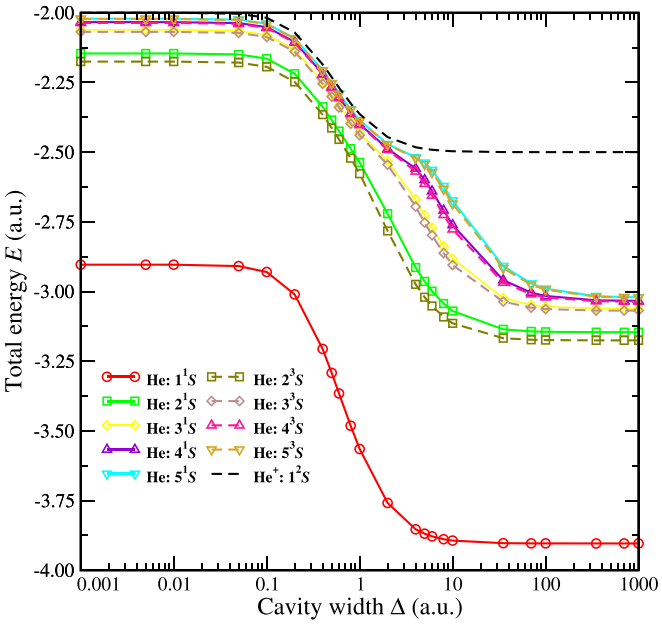

FIG. 1. Variation of energy eigenvalues E of He ($1sns$, ^1S) ($n = 1-5$) (solid lines), He ($1sns$, ^{3}S) ($n = 2-5$) (dashed lines) and He^+ ($1s$, ^2S) (black dashed line) with respect to cavity width Δ. Cavity depth V_0 is fixed at 0.5. All entities are in a.u.

same for $V_0 = 1.0$ a.u. and the same argument is found to be true for this case also. The detailed variation of the FO potential energy E_c with respect to Δ for constant $V_0 = 0.5$ a.u. corresponding to the ground and singly excited $1sns$ ($^{1,3}S$) ($n = 2-5$) states of He atoms is depicted in Fig. 2(b). It may be concluded that the overall variation of the total energy is actually controlled by the energy component due to the confining FO potential E_c.

B. Hund's rule and the electron repulsion energy

The set of three Hund's spin multiplicity rules were proposed empirically in a series of publications [102–105] prior to the beginning of the era of new quantum mechanics. In this section, we are concerned with the first spin multiplicity rule which states that for a given atomic open shell electronic configuration, the term with the maximum spin multiplicity corresponds to the lowest energy. Slater [106], using the first-order perturbation theory along with the assumption of the common set of frozen orbitals for the multiplets, showed that the stability of the higher spin multiplet originated from the lowering of interelectronic repulsion due to the exchange stablization. However, the assumption of the frozen orbitals common to all the multiplets gives rise to the different terms having a common kinetic energy but different total energies, which violates the virial theorem. Davidson [107] studied the singly excited states of He within the Hartree-Fock framework, in which the orbitals are optimized, individually, for a total of 18 terms (singlet and triplet), thus including the variationally relaxed orbitals within the theoretical analysis. This work concluded with a remarkably intriguing observation: "In every case, however, the electron-repulsion integral is larger for the triplet than for the singlet. Thus it is not true, as is usually assumed, that the triplet lies lower because it has less electron repulsion." Subsequently, several studies on different atoms and QDs have been reported [107–115] which suggest that while the Hund's rule remains valid in such systems, the relative ordering of the electron-repulsion integral can actually be either larger or smaller in the higher spin multiplet. We shall now present the results of our calculations on the He atom in the QD modeled by Eq. (1) with reference to the validity of the Hund's rule, in general, for the configuration He ($1sns$) with $n = 2-5$. Special consideration will be given to the ^1S and ^3S states originating from the He ($1sns$) configuration in analyzing the electron-electron interaction vis-à-vis the difference in the total energy of the ^3S and ^1S states. In Fig. 1, we have displayed the total energy, E, versus the cavity width, Δ, for the ^1S and ^3S states arising from the He ($1sns$) with $n = 2-5$. It is observed that at all values of Δ, the ^3S state is always lower than the ^1S state, as predicted by the Hund's spin multiplicity rule. The magnitude of the singlet-triplet total energy difference decreases as n increases for the excited He ($1sns$). This result is similar to those reported for the He atom in the free [107] and the screened Coulomb potential [114,115]. In Fig. 3, we have shown the variation of the difference between the electron-repulsion energy, $[\langle\frac{1}{r_{12}}\rangle_{^3S} - \langle\frac{1}{r_{12}}\rangle_{^1S}]$, with the cavity width Δ. We report the interesting result that in each case of the ^3S and ^1S arising out of He ($1sns$) with $n = 2-5$ configuration, there exist three ranges of Δ as marked in Fig. 3, over which the ordering of the electronic repulsion energy given by (i) $\langle\frac{1}{r_{12}}\rangle_{^3S} > \langle\frac{1}{r_{12}}\rangle_{^1S}$, (ii) $\langle\frac{1}{r_{12}}\rangle_{^3S} < \langle\frac{1}{r_{12}}\rangle_{^1S}$, (iii) $\langle\frac{1}{r_{12}}\rangle_{^3S} > \langle\frac{1}{r_{12}}\rangle_{^1S}$, respectively. In all these cases, the virial theorem dictates that the total potential energy corresponding to the triplet state is more negative than the singlet state. This underscores the important role played by the nuclear attraction term in determining the overall stability of the triplet state at all values of the cavity width Δ. To the best of our knowledge, the He atom in a QD described by the FO potential given by Eq. (1) represents a model potential which exhibits both higher and lower electron repulsion in the higher spin multiplet as the parameter Δ of the potential is continuously varied over which the total energy of the higher spin state is always lying below the lower spin multiplet.

The FO potential in Eq. (1) at fixed V_0 is characterized by the cavity width Δ. At large values of Δ, the FO potential is very wide, so the electrons in the He impurity interact only feebly because they are localized by the Coulomb potential. At small values of Δ, the FO potential is too narrow and its effect diminished again since the electrons in the He impurity interact with it when they are very close to the nucleus, a region where the radial probability vanishes (because of the volume element, that depends on r^2). As a consequence, in Fig. 3, at the two limiting values Δ, the variation of the difference $\langle\frac{1}{r_{12}}\rangle_{^3S} - \langle\frac{1}{r_{12}}\rangle_{^1S}$ is found to be nearly similar with $\langle\frac{1}{r_{12}}\rangle_{^3S} > \langle\frac{1}{r_{12}}\rangle_{^1S}$. The latter order of the electron repulsion is similar to the free He atom.

At the intermediate range of Δ, the FO potential induces a reversal of the relative magnitudes of the singlet versus triplet interelectronic repulsions. This specific behavior of the singlet versus triplet interelectronic repulsions along the He isoelectronic sequence is indeed observed [115] at larger Z

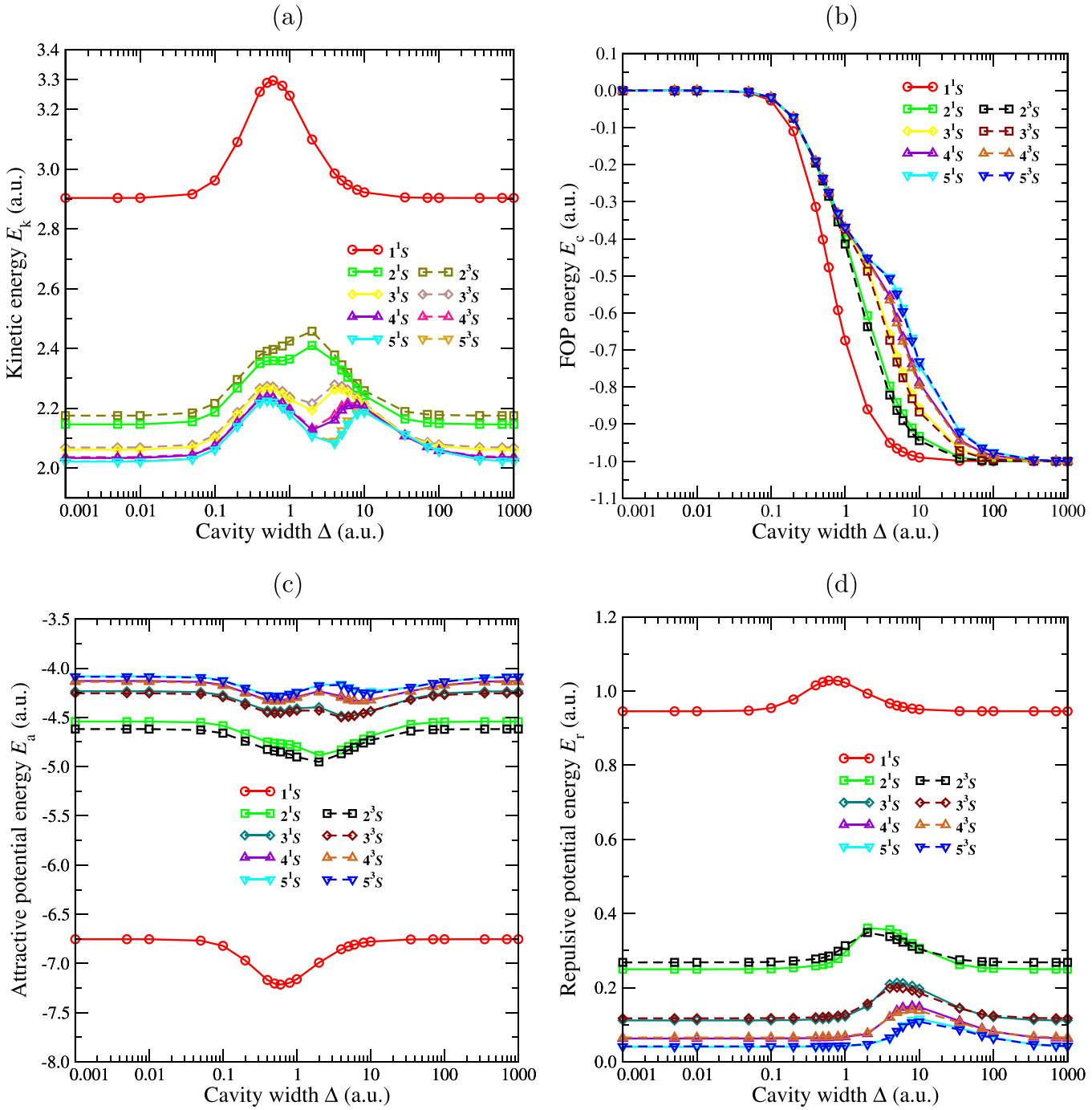

FIG. 2. Variation of (a) kinetic energy E_k, (b) FOP energy E_c, (c) attractive potential energy E_a, (d) repulsive potential energy E_r corresponding to He in $1sns$ (^1S) ($n = 1 - 5$) states (solid lines) and $1sns$ (^{3}S) ($n = 2 - 5$) states (dashed lines) with respect to cavity width Δ. Cavity depth V_0 is fixed at 0.5. All entities are in a.u.

values wherein the interelectronic repulsion is higher in the singlet. This higher-Z behavior is in agreement with first-order perturbation theory, where $1/Z = 0$ ($Z =$ infinity) is taken as the zero-order Hamiltonian. In this limit, the interelectronic repulsion is $J + K$ for the singlet and $J - K$ for the triplet, both the Coulomb integral, J, and the exchange integral K being positive.

On the basis of this observation, we conclude that the cavity width Δ of the FO potential in the intermediate range given in Fig. 3 enhances the one-body attraction to the nucleus thus acting in the same way as observed in the He series at higher Z values in the free state.

C. Variation of correlation energy

The estimation of total correlation energy leads to understanding the nonlocality of the electrons and also it is related to the quantum entanglement [57]. The total correlation energy E_{corr} can be estimated by subtracting Hatree-Fock energy E_{HF} from the energy obtained with explicitly correlated

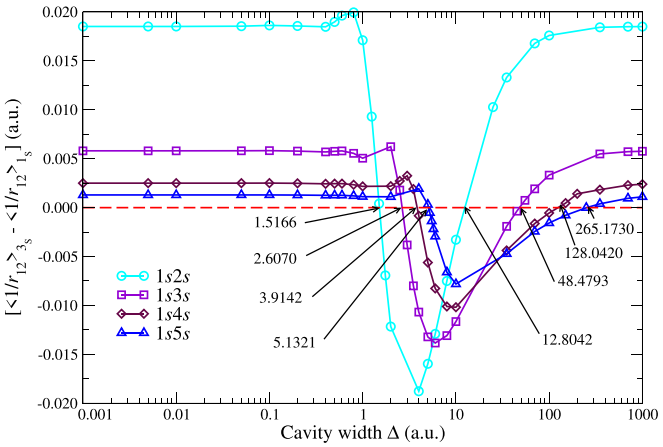

FIG. 3. Variation of $[\langle\frac{1}{r_{12}}\rangle_{^3S} - \langle\frac{1}{r_{12}}\rangle_{^1S}]$ corresponding to He in $1sns$ ($^{1,3}S$) ($n = 2 - 5$) states with respect to cavity width Δ. Cavity depth V_0 is fixed at 0.5. All entities are in a.u.

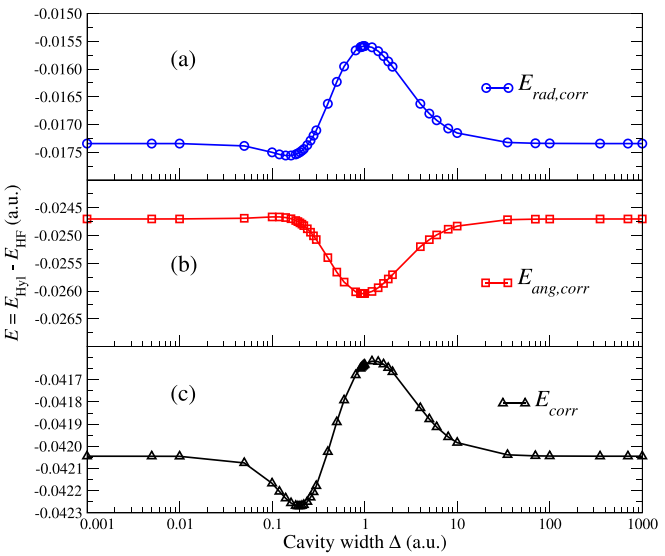

FIG. 4. Variation of (a) radial correlation limit of total correlation energy $E_{\text{rad,corr}}$ (○, blue line), (b) angular correlation limit of total correlation energy $E_{\text{ang,corr}}$ (□, red line), and (c) the total correlation energy E_{corr} (Δ, black line) corresponding to the ground state of He with respect to cavity width Δ. Cavity depth V_0 is fixed at 0.5. All entities are in a.u.

Hylleraas type wave function E_{Hyl} as

$$E_{\text{corr}} = E_{\text{Hyl}} - E_{\text{HF}}. \tag{12}$$

The component of radial $E_{\text{rad,corr}}$ and angular $E_{\text{ang,corr}}$ correlations in the total correlation energy have been determined as

$$\begin{aligned} E_{\text{rad,corr}} &= E_{\text{Hyl}}^{\text{rad}} - E_{\text{HF}}, \\ E_{\text{ang,corr}} &= E_{\text{Hyl}} - E_{\text{Hyl}}^{\text{rad}}, \end{aligned} \tag{13}$$

where the energy $E_{\text{Hyl}}^{\text{rad}}$ is obtained in the absence of any r_{12} term in the wave function defined in Eq. (5).

A detailed study on the E_{corr}, $E_{\text{rad,corr}}$, and $E_{\text{ang,corr}}$ separately in the total energy have been performed for the ground state of the confined He atom. The variations of E_{corr} (black line), $E_{\text{rad,corr}}$ (blue line), and $E_{\text{ang,corr}}$ (red line) with respect to cavity width Δ corresponding to cavity depth $V_0 = 0.5$ a.u. has been demonstrated in Fig. 4. It can be noted that the value of E_{corr} has a decreasing trend for smaller values of Δ and after which it has a sharp peak around $\Delta = 1.0$ a.u. The exactly opposite nature of the energy contribution from $E_{\text{rad,corr}}$ and $E_{\text{ang,corr}}$ are clearly visualized in Fig. 4. In Table III, we have listed some of our estimated results of E_{corr}, $E_{\text{rad,corr}}$, and $E_{\text{ang,corr}}$ for different sets of (V_0, Δ). It is observed that E_{corr} remains almost constant up to $\Delta = 0.05$ a.u. The contribution of the E_{corr} within this region is almost 1.45% of the total energy and the maximum part of this correlation comes from the $E_{\text{ang,corr}}$, which is almost 58.75% of the E_{corr}. At $\Delta = 0.2$ a.u., E_{corr} takes the minimum value i.e., -0.04226946 a.u. and at that point the value of $E_{\text{ang,corr}}$ is -0.02477133 a.u. which is 58.60% of E_{corr}. Beyond $\Delta = 0.2$ a.u., E_{corr} has a smooth transition within which E_{corr} decreases rapidly and the value of E_{corr} becomes -0.04164917 a.u. at $\Delta = 0.9$ a.u. Up to $\Delta = 0.9$ a.u. the $E_{\text{ang,corr}}$ increases monotonically and then it saturates to the value -0.02470162 a.u. for $\Delta = 1000.0$ a.u. by making 58.75% contribution in E_{corr}. In contrast, up to $\Delta = 0.9$ a.u., $E_{\text{rad,corr}}$ decreases fast which becomes -0.01560716 a.u. at $\Delta = 0.9$ a.u. with 37.47% contribution in E_{corr} and after that it saturates to the value -0.01734276 a.u. with 41.25% contribution in E_{corr}. The interplay between $E_{\text{ang,corr}}$ and $E_{\text{rad,corr}}$ in E_{corr} is therefore very interesting in the region of cavity width $\Delta = 0.1 - 10$ a.u. for the cavity depth fixed at $V_0 = 0.5$ a.u.

D. Entanglement entropy

The linear entropy S_L and von Neumann entropy S_{vN} in terms of reduced density matrix ρ_{red} are defined as follows

TABLE III. Hatree-Fock energy E_{HF}, total correlation energy E_{corr}, radial correlation energy $E_{\text{rad,corr}}$ and angular correlation energy $E_{\text{ang,corr}}$ corresponding to the ground state of He for different cavity widths Δ and cavity depths V_0. All entities are in a.u

V_0	Δ	$-E_{\text{HF}}$	$-E_{\text{corr}}$	$-E_{\text{rad,corr}}$	$-E_{\text{ang,corr}}$
0.0	–	2.86168000	0.04204440	0.01734279	0.02470161
0.5	0.001	2.86168006	0.04204434	0.01734279	0.02470155
	1.0	3.52327365	0.04163105	0.01558573	0.02604532
	1000.0	3.86167881	0.04204439	0.01734276	0.02470162
1.0	0.001	2.86168035	0.04204438	0.01734279	0.02470159
	1.0	4.42190798	0.04143363	0.01460633	0.02682730
	1000.0	4.86167881	0.04204437	0.01734276	0.02470161

TABLE IV. Convergence of von Neumann entropy S_{vN} and linear entropy S_L corresponding to the ground state of He atom with respect to $l_{\max}$ for $n_{\max} = 100$ and 200. The cavity width Δ and cavity depth V_0 are set at 1.0 and 0.5, respectively. All entities are in a.u.

	$n_{\max} = 100$		$n_{\max} = 200$	
$l_{\max}$	S_{vN}	S_L	S_{vN}	S_L
0	0.03493860	0.01496846	0.03386940	0.01343357
1	0.07136378	0.01496422	0.07029066	0.01342933
2	0.07397524	0.01496421	0.07290078	0.01342932
4	0.07453588	0.01496421	0.07346006	0.01342932
6	0.07459150	0.01496421	0.07351505	0.01342932
8	0.07460262	0.01496421	0.07352584	0.01342932
10	0.07460586	0.01496421	0.07352890	0.01342932

[48,49,54,55]:

$$S_{vN} = -\mathrm{Tr}(\rho_{\mathrm{red}} \log_2 \rho_{\mathrm{red}}); \quad S_L = 1 - \mathrm{Tr}\left(\rho_{\mathrm{red}}^2\right), \tag{14}$$

where the reduced density matrix of a two-electron system is defined as $\rho_{\mathrm{red}} = |\Psi\rangle\langle\Psi|$. The eigenvalues of the reduced density matrix ρ_{red} have been estimated with the aid of Schmidt decomposition method [63,116,117]. Specifically, the von Neumann entropy and the Linear entropy can be written in terms of λ_{nl} (the eigenvalue of the reduced density matrix) as follows:

$$S_{vN} = -\sum_{nlm} \lambda_{nl} \log_2 (\lambda_{nl}); \quad S_L = 1 - \sum_{nlm} (\lambda_{nl})^2. \tag{15}$$

Since the value of m runs from $-l$ to $+l$ i.e., $2l + 1$ degenerate values, the above two equations can be modified as

$$S_{vN} = -\sum_{nl} (2l+1)\lambda_{nl} \log_2 (\lambda_{nl});$$
$$S_L = 1 - \sum_{nl} (2l+1)(\lambda_{nl})^2. \tag{16}$$

The numerical procedure used here to compute the von Neumann and the linear entropy has been explained in detail by Kóscik [70].

The von Neumann entropy S_{vN} and the linear entropy S_L corresponding to He ($1s^2$, ^1S) and He ($1s2s$, ^1S) have been estimated with $N = 34$ and 50 terms, respectively, in the Hyllerass-type basis set. The upper limits ($l_{\max}$ and $n_{\max}$) in the summation of Eq. (16) are increased to attain a desired level of accuracy. We have changed $l_{\max}$ from 0 to 10 by fixing $n_{\max}$ with 100 and 200, respectively. In Table IV, the convergence in S_{vN} and S_L with respect to $l_{\max}$ and $n_{\max}$ is listed. The values of S_{vN} and S_L in the second and third column of Table IV are given for $n_{\max} = 100$ while the fourth and fifth columns of same are given for $n_{\max} = 200$. The present result shows qualitative agreement with the available results [48–55,60,70,71] which can be seen from Table V. Table V depicts some representative estimates of S_{vN} and S_L corresponding to He ($1s^2$, ^1S) and He ($1s2s$, ^1S) with $l_{\max} = 10$ and $n_{\max} = 200$ for different sets of (V_0, Δ). It can be seen that for a constant value of V_0, the value of S_{vN} and S_L corresponding to He ($1s^2$, ^1S) and He ($1s2s$, ^1S) of He atoms have a sharp minimum with respect to the cavity width Δ. The detailed variation of the S_{vN} and S_L with respect to cavity width Δ for fixed value of $V_0 = 0.5$ a.u. is plotted for the ground state of a confined He atom, given in Fig. 5.

E. Variation of geometrical properties

By computing the optimal variational parameters α_i and β_i and the linear coefficients C_i of the wave function Ψ defined in Eq. (5), we have estimated different geometrical properties of the confined He atom, namely, the expectation value of inter-particle distances i.e., radial moments $\langle r_1 \rangle$, $\langle r_{12} \rangle$, $\langle r_1^2 \rangle$, and $\langle r_{12}^2 \rangle$, expectation value of interparticle angles i.e., angular moments $\langle \theta_1 \rangle$ and $\langle \theta_{12} \rangle$ with the same order of accuracy as described for energy. Furthermore, we have evaluated the

TABLE V. The von Neumann entropy S_{vN} and the Linear entropy S_L corresponding to ($1s^2$, ^1S) and ($1s2s$, ^1S) states of He for different cavity widths Δ and cavity depths V_0. [$l_{\max} = 10$ and $n_{\max} = 200$]. All entities are in a.u. *a*: Lin and Ho [60], *b*: Dehesa *et al.* [48,49], *c*: Benenti *et al.* [50], *d*: Lin *et al.* [51], *e*: Lin *et al.* [52], *f*: Lin and Ho [55], *g*: Kościk and Okopińska [54], *h*: Hofer [53], *i*: Kościk [70].

		$1s^2$, ^{1}S		$1s2s$, ^{1}S	
V_0	Δ	S_{vN}	S_L	S_{vN}	S_L
Free		0.08497	0.01601	0.99203	0.48899
		0.084998[a]	0.015937[a]	0.991917[a]	0.488737[a]
			0.015914[b]		0.48866[b]
		0.0785[c]	0.01606[c]	0.991099[c]	0.48871[c]
			0.015943[d]		0.488736[d]
			0.0159156[e]		
		0.08489987[f]	0.01591564[f]	0.99191721[f]	0.48874040[f]
		0.0848999[g]	0.0159157[g]		
		0.06749889[h]	0.01595052[h]		
			0.0159172[i]		
0.5	0.001	0.08497	0.01601	0.99211	0.48921
	1.0	0.07353	0.01343	0.99554	0.49016
	1000.0	0.08497	0.01601	0.99211	0.48920
1.0	0.001	0.08497	0.01601	0.99211	0.48921
	1.0	0.06860	0.01235	0.99882	0.48706
	100.0	0.08497	0.01601	0.99211	0.48920

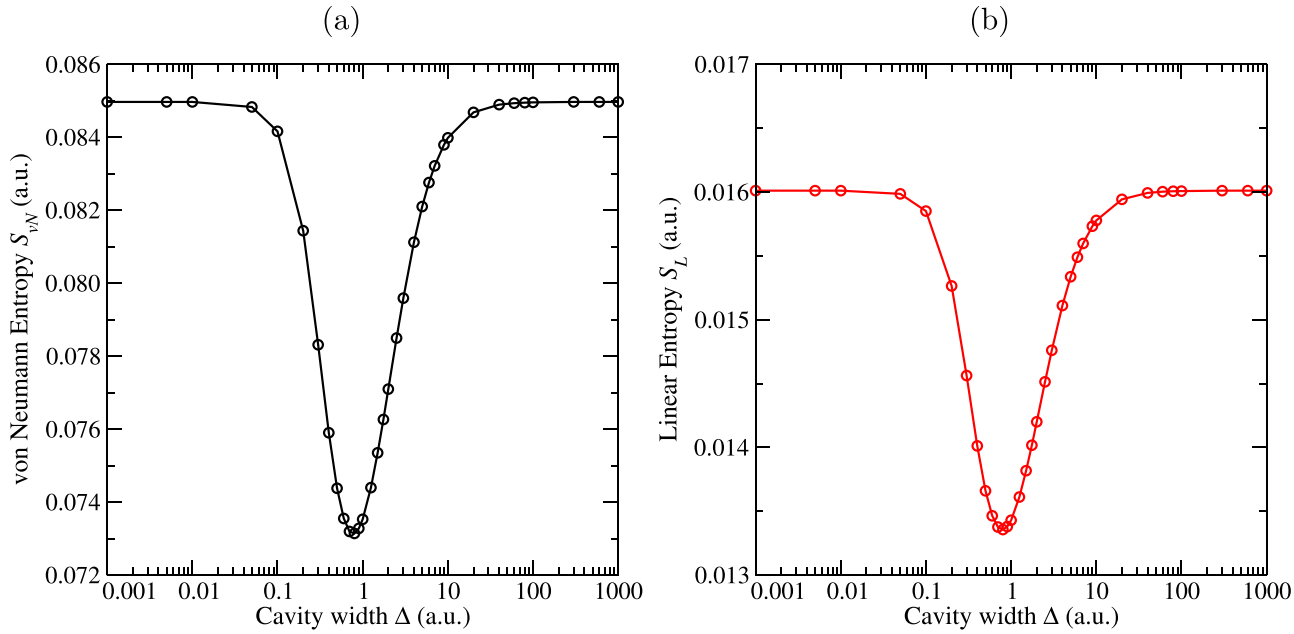

FIG. 5. Variation of (a) von Neumann entropy S_{vN}, (b) linear entropy S_L corresponding to the ground state of He with respect to cavity width Δ. Cavity depth V_0 is fixed at 0.5. All entities are in a.u.

expectation value of the inner radius $r_< = \min(r_1, r_2)$ and the outer radius $r_> = \max(r_1, r_2)$ [42,118,119]. The two-electron He atom always prefers two different radii $r_<$ and $r_>$ at any instant of time [120,121] to minimize the electron-electron repulsion effect. The expectation value of electron-electron delta function $\delta(\vec{r}_{12})$ and electron-nuclear delta function $\delta(\vec{r}_1)$ have also been estimated in this paper. We have listed all results up to eight decimal places.

In Tables VI and VII, we have, respectively, listed the one-particle and two-particle radial moments [$\langle r_1\rangle$, $\langle r_1^2\rangle$, $\langle r_{12}\rangle$, $\langle r_{12}^2\rangle$], the angular moments ($\langle\theta_1\rangle$, $\langle\theta_{12}\rangle$) along with the delta functions [$\langle\delta(\vec{r}_1)\rangle$, $\langle\delta(\vec{r}_{12})\rangle$] for different cavity parameters (V_0, Δ). The respective structural properties of the ground and $1s2s$ (^3S) states of the free He atom is listed in the first row of Tables VI and VII. It is observed that for a specific value of V_0, the radial moments (i.e., $\langle r_1\rangle$, $\langle r_1^2\rangle$, $\langle r_{12}\rangle$, and $\langle r_{12}^2\rangle$) of ground and singly excited states of He atoms are insensitive for lower values of Δ, but the system starts to squeeze as the value of Δ reaches 0.1 a.u. Interestingly, the rate of such squeezing increases rapidly up to a certain limit of Δ (say, Δ_m), beyond which the system again starts to expand and for large values of Δ, the system again behaves the same as the free one. It is also worthwhile to note that the value of Δ_m moves toward the higher region as we consider the singly excited state. In particular, the value of Δ_m is ≈0.8 a.u. for the ground state of the He atom, which rises to ≈2 a.u. in case of singlet or triplet $1s2s$ state of He atom. Besides, there is a distinct minimum for ground state and lower singly excited state, which vanishes for higher singly excited states. Figures 6 and 7 clearly depict the variation of different radial moments for different sets of (V_0, Δ) and it can be noted that for all singly excited states, the value of radial moments of a singly excited singlet state always remains greater as compared to the respective triplet state irrespective of any value of V_0 and Δ. The detailed variation of the one- and two-electron angular moments corresponding to ground and $1s2s$ (^3S) states of He atoms for different V_0 and Δ are clearly illustrated in Fig. 8. We find unique characteristics [shown in Fig. 8(a)] of the electron-nucleus angular moment of ground state of He atom in which we have observed a sharp transition from

TABLE VI. Variation of one-particle radial moments $\langle r_1\rangle$, $\langle r_1^2\rangle$ (a.u.), one-particle angular moment $\langle\theta_1\rangle$ (degree), and one-particle delta function $\langle\delta(\vec{r}_1)\rangle$ (a.u.) corresponding to ($1s^2$, ^1S) and ($1s2s$, ^3S) states of He for different cavity widths Δ (a.u.) and cavity depths V_0 (a.u.).

		$1s^2$, ^1S				$1s2s$, ^3S			
V_0	Δ	$\langle r_1\rangle$	$\langle r_1^2\rangle$	$\langle\theta_1\rangle$	$\langle\delta(\vec{r}_1)\rangle$	$\langle r_1\rangle$	$\langle r_1^2\rangle$	$\langle\theta_1\rangle$	$\langle\delta(\vec{r}_1)\rangle$
0.0	–	0.92947229	1.19348300	49.608	1.81042767	2.55046268	11.46432162	55.751	1.32035503
0.5	0.001	0.92947228	1.19348295	49.608	1.81042617	2.55046265	11.46432140	55.751	1.32035551
	1.0	0.85747304	0.99651065	49.528	2.01752780	2.20999955	8.41731367	55.372	1.45036235
	1000.0	0.92947153	1.19348046	49.608	1.81042636	2.55032861	11.46277122	55.751	1.32036129
1.0	0.001	0.92947219	1.19348275	49.608	1.81043281	2.55046251	11.46432037	55.751	1.32035774
	1.0	0.82451242	0.90896844	49.463	2.10948066	1.76560504	4.96954520	54.550	1.56787612
	1000.0	0.92947153	1.19348046	49.608	1.81042750	2.55032826	11.46276696	55.751	1.32036140

TABLE VII. Variation of two-particle radial moments $\langle r_{12}\rangle$, $\langle r_{12}^2\rangle$ (a.u.), two-particle angular moment $\langle\theta_{12}\rangle$ (degree), and two-particle delta function $\langle\delta(\vec{r}_{12})\rangle$ (a.u.) corresponding to ($1s^2$, ^1S) and ($1s2s$, ^3S) states of He for different cavity widths Δ (a.u.) and cavity depths V_0 (a.u.).

		$1s^2$, ^1S				$1s2s$, ^3S			
V_0	Δ	$\langle r_{12}\rangle$	$\langle r_{12}^2\rangle$	$\langle\theta_{12}\rangle$	$\langle\delta(\vec{r}_{12})\rangle$	$\langle r_{12}\rangle$	$\langle r_{12}^2\rangle$	$\langle\theta_{12}\rangle$	$\langle\delta(\vec{r}_{12})\rangle$
0.0		1.42207026	2.51643931	93.681	0.10677637	4.44753522	23.04619748	90.908	0.0
0.5	0.001	1.42207023	2.51643922	93.681	0.10677768	4.44753517	23.04619702	90.908	0.0
	1.0	1.30427403	2.10119584	93.588	0.13223847	3.80916589	16.93851119	90.998	0.0
	1000.0	1.42206896	2.51643408	93.681	0.10677784	4.44727274	23.04309951	90.908	0.0
1.0	0.001	1.42207009	2.51643876	93.681	0.10677771	4.44753496	23.04619494	90.908	0.0
	1.0	1.24994803	1.91777046	93.563	0.14511388	2.96409633	10.03964514	91.255	0.0
	1000.0	1.42206896	2.51643408	93.681	0.10677783	4.44727204	23.04309100	90.908	0.0

maximum to a minimum value as Δ increases for a specific value of V_0. The value of $\langle\theta_1\rangle$ corresponding to ground state of a He atom with $V_0 = 0.5$ a.u. increases monotonically to 49.652° at $\Delta = 0.2$ a.u. and thereafter it decreases rapidly to the value 49.50° at $\Delta = 2.0$ a.u., beyond which it increases smoothly and converges to the value 49.588° for high Δ. In contrast, for singly excited singlet or triplet states of He atoms, both $\langle\theta_1\rangle$ and $\langle\theta_{12}\rangle$ have a distinct maxima within the Δ value 0.1 a.u. and 10.0 a.u. Further, it is also apparent from Fig. 8 that there are two distinct points of Δ, one below Δ_m and the other above Δ_m, at which the value of $\langle\theta_1\rangle$ is the same for both singly excited singlet and triplet states of He atoms. For the $1s2s$ state, these two points are at approximately 2.0 a.u. and 6.0 a.u., which increases to approximately 5.0 a.u. and 100.0 a.u. for the $1s5s$ state of the He atom. Similar characteristics of $\langle\theta_{12}\rangle$ can also be noticed in Fig. 8(b), but in that case we observed a sharp maxima with in the Δ range [0.1,10.0] a.u.

The influence of the FO potential on one-electron delta function $\langle\delta(\vec{r}_1)\rangle$ corresponding to ground state and singly excited singlet and triplet states of He atoms is very much prominent and we have noticed a sharp maximum for the same with in the approximate Δ range [0.1,10] a.u. Unlike this, the two-electron delta function $\langle\delta(\vec{r}_{12})\rangle$ of the singly excited triplet state of a He atom always remains zero irrespective of any value of V_0 and Δ. In Fig. 9, we have shown the variation of $\langle\delta(\vec{r}_1)\rangle$ and $\langle\delta(\vec{r}_{12})\rangle$ corresponding to ground and singly excited states of He atoms for different values of Δ by fixing the V_0 at 0.5 a.u.

The variation of the inner radius expectation value $\langle r_<\rangle$ and outer radius expectation value $\langle r_>\rangle$ corresponding to the ground state and $1s2s$ (^3S) of He atoms under FO potential are summarized in Table VIII. It is clear from the results that the inner radius $\langle r_<\rangle$ and the outer radius $\langle r_>\rangle$ are being modified in the presence of the FO potential. Moreover, the values of $\langle r_<\rangle$ and $\langle r_>\rangle$ are greater for smaller V_0, corresponding to a specific value of Δ, and the behavior of $\langle r_<\rangle$ and $\langle r_>\rangle$, corresponding to different excited states of He atoms are the same as for the ground state of a He atom. Although the values of $\langle r_<\rangle$ and $\langle r_>\rangle$ are always greater for the upper excited state as compared to the lower one. To view this, we have listed some representative values of $\langle r_<\rangle$ and $\langle r_>\rangle$ for the $1s2s$ (^3S) state of He atoms in Table VIII. Figure 10 also depicts the variation of $\langle r_<\rangle$ and $\langle r_>\rangle$ for different values of Δ but with $V_0 = 0.5$ a.u. It can be observed that the value of $\langle r_<\rangle$ is minimum (≈ 0.562 a.u.) at around $\Delta = 1.0$ a.u. and at around that point the minimum value of $\langle r_>\rangle$ is (≈ 1.145 a.u.). The variation of $\langle r_<\rangle$ corresponding to the singlet $1sns$ ($n = 2 - 5$) states of He atom with respect to Δ are very closely spaced but in the case of triplet states, the variations are distinct and stay below the singlet state. In contrast, the variation of $\langle r_>\rangle$ for singly excited singlet and triplet states of He atoms are very much distinct. The variation of $\langle r_>\rangle$ of a particular triplet state changes in the same way as a singlet state but the value corresponding to the singlet state is always larger as compared to the respective triplet state.

F. Hellmann-Feynman and virial theorems

The Hellmann-Feynman and virial theorems have been verified for both a He atom in ground state and its first ionization threshold, i.e., $He^+(1s)$ ion.

TABLE VIII. Expectation value of inner radius $r_<$ and outer radius $r_>$ corresponding to ($1s^2$, ^1S) and ($1s2s$, ^3S) states of He for different cavity widths Δ and cavity depths V_0. All entities are in a.u.

		$1s^2$, ^1S		$1s2s$, ^3S	
V_0	Δ	$\langle r_<\rangle$	$\langle r_>\rangle$	$\langle r_<\rangle$	$\langle r_>\rangle$
0.0	–	0.60235942	1.25658517	0.72946094	4.37146441
0.5	0.001	0.60235940	1.25658515	0.72946093	4.37146437
	1.0	0.56673911	1.14820699	0.68843973	3.73155937
	1000.0	0.60235914	1.25658392	0.72945833	4.37119889
1.0	0.001	0.60235934	1.25658504	0.72946085	4.37146417
	1.0	0.55162689	1.09739795	0.65414828	2.87706181
	1000.0	0.60235914	1.25658394	0.72945832	4.37119819

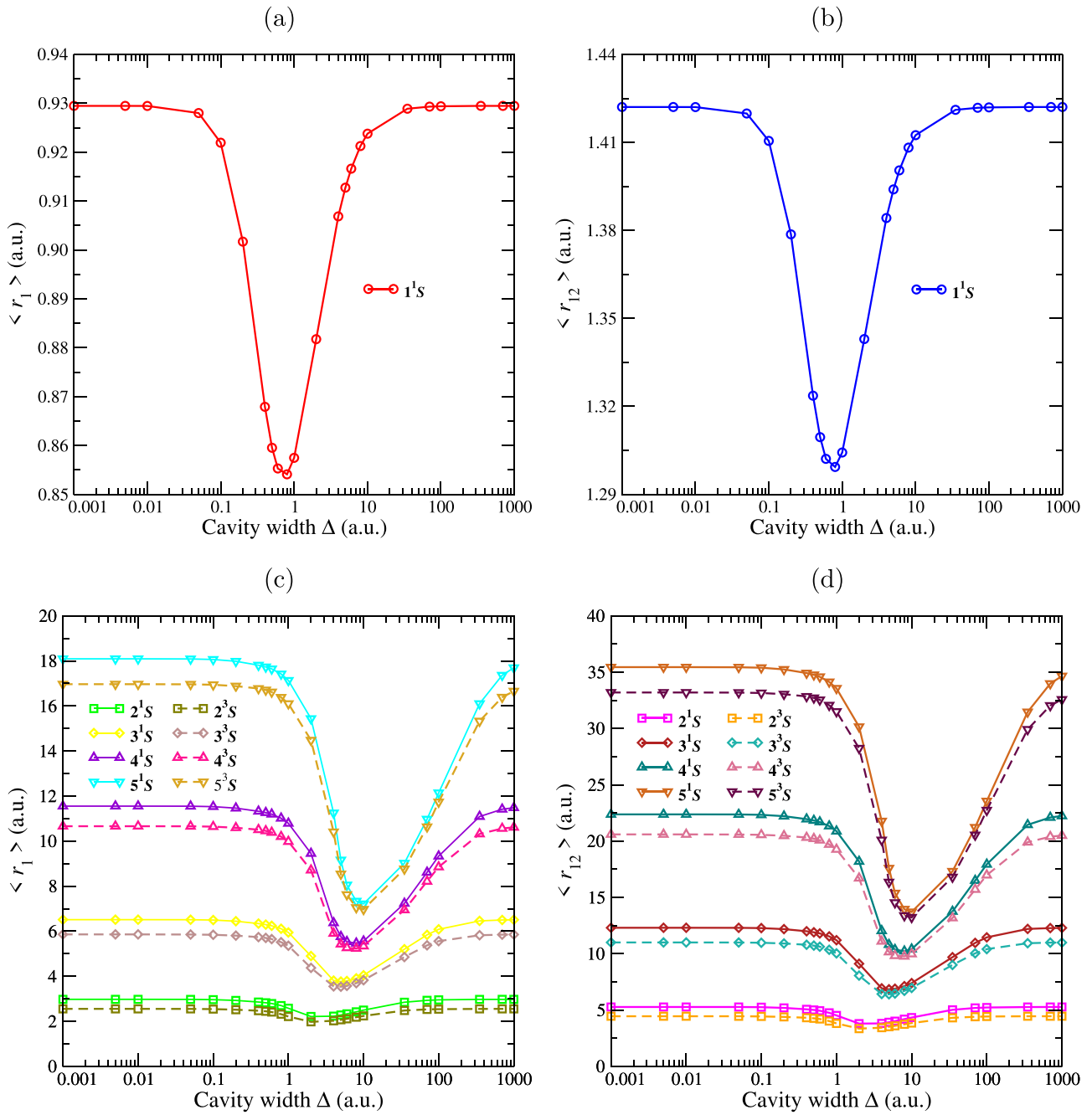

FIG. 6. Variation of (a) one-electron radial moment $\langle r_1 \rangle$ of He in ground state, (b) two-electron radial moment $\langle r_{12} \rangle$ of He in ground state, (c) one-electron radial moment $\langle r_1 \rangle$ of He in $1sns$ (^1S) ($n = 2 - 5$) states (solid lines) and in $1sns$ (^3S) ($n = 2 - 5$) states (dashed lines), (d) two-electron radial moment $\langle r_{12} \rangle$ of He in $1sns$ (^1S) ($n = 2 - 5$) states (solid lines) and in $1sns$ (^3S) ($n = 2 - 5$) states (dashed lines) with respect to cavity width Δ. Cavity depth V_0 is fixed at 0.5. All entities are in a.u.

1. He atom

Hamiltonian of He atom under FO potential defined in Eq. (1) can be written as

$$H = T + V_1^c + V_{12}^c + V_{cw} = T + V_t^c + V_{cw}, \tag{17}$$

where $T = -\sum_{i=1}^{2} \frac{1}{2}\nabla_i^2$, $V_1^c = -\sum_{i=1}^{2} \frac{Z}{r_i}$, $V_{12}^c = \frac{1}{r_{12}}$ and $V_{cw} = -\sum_{i=1}^{2} V_0(1 + c_w r_i)e^{-c_w r_i}$. If ϕ is the eigenvector and corresponding eigenvalue e, then we can define $t = \langle T \rangle$, $v_1^c = \langle V_1^c \rangle$, $v_{12}^c = \langle V_{12}^c \rangle$, $v_t^c = \langle V_1^c + V_{12}^c \rangle$, and $v_{cw} = \langle V_{cw} \rangle$. Thus, the total energy eigenvalue can be written as

$$e = t + v_1^c + v_{12}^c + v_{cw} = t + v_t^c + v_{cw}. \tag{18}$$

The Hellmann-Feynman theorem with respect to Δ gives

$$u = \frac{\Delta}{V_0}\frac{de}{d\Delta}, \tag{19}$$

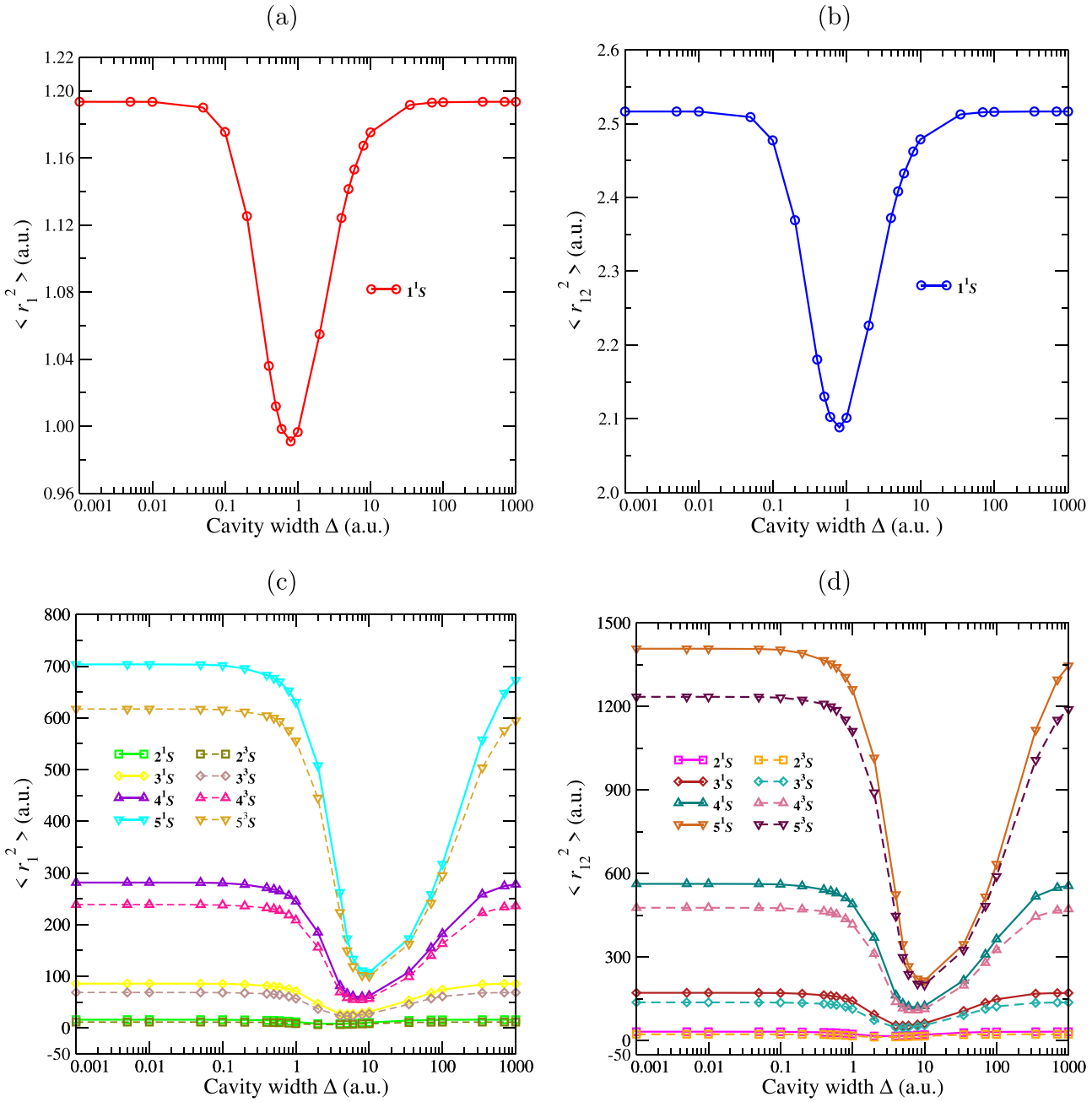

FIG. 7. Variation of (a) one-electron radial moment $\langle r_1^2 \rangle$ of He in ground state, (b) two-electron radial moment $\langle r_{12}^2 \rangle$ of He in ground state, (c) one-electron radial moment $\langle r_1^2 \rangle$ of He in $1sns$ (^1S) ($n = 2 - 5$) states (solid lines) and in $1sns$ (^3S) ($n = 2 - 5$) states (dashed lines), (d) two-electron radial moment $\langle r_{12}^2 \rangle$ of He in $1sns$ (^1S) ($n = 2 - 5$) states (solid lines) and in $1sns$ (^3S) ($n = 2 - 5$) states (dashed lines) with respect to cavity width Δ. Cavity depth V_0 is fixed at 0.5. All entities are in a.u.

where, $u = -c_w^2 \langle [r_1^2 e^{-c_w r_1} + r_2^2 e^{-c_w r_2}] \rangle$. Using Eq. (19), Hellmann-Feynman theorem with respect to V_0 gives

$$v_{cw} = V_0 \frac{de}{dV_0} - \frac{\Delta}{2} \frac{de}{d\Delta} \tag{20}$$

and the Hellmann-Feynman theorem with respect to Z gives

$$v_1^c = Z \frac{de}{dZ}. \tag{21}$$

Therefore, from the virial theorem, it is quite straightforward to show that

$$2t + v_t^c = -\Delta \frac{de}{d\Delta}. \tag{22}$$

Therefore, using Eq. (18) and Eq. (20), Eq. (22) can be recast as

$$t = V_0 \frac{de}{dV_0} - \frac{3}{2} \Delta \frac{de}{d\Delta} - e. \tag{23}$$

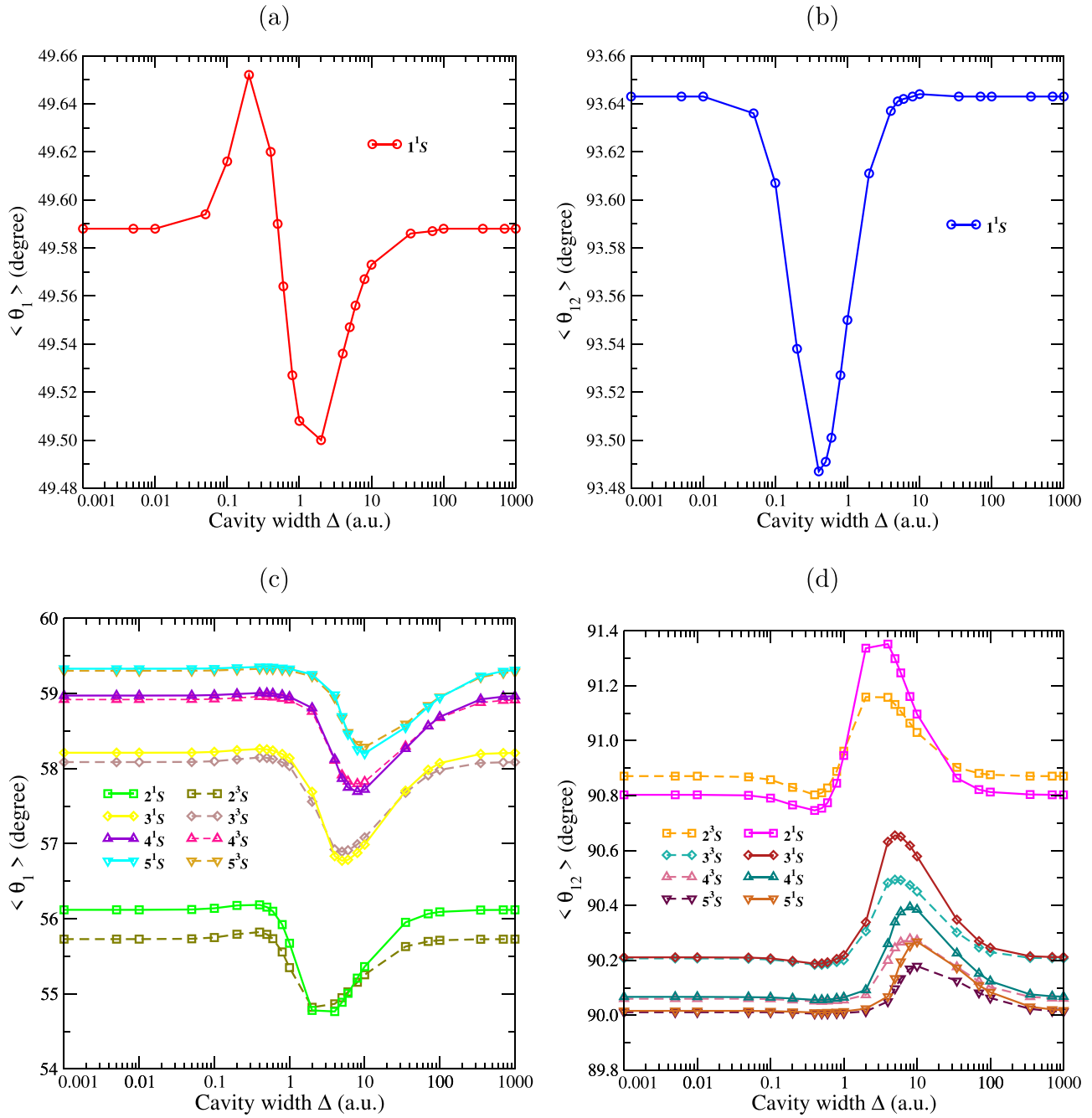

FIG. 8. Variation of (a) nucleus-electron angle $\langle\theta_1\rangle$ (degree) of He in ground state, (b) interelectronic angle $\langle\theta_{12}\rangle$ (degree) of He in ground state, (c) nucleus-electron angle $\langle\theta_1\rangle$ (degree) of He in $1sns$ (^1S)($n = 2-5$) states (solid lines) and in $1sns$ (^3S) ($n = 2-5$) states (dashed lines), (d) inter electronic angle θ_{12} (degree) of He in $1sns$ (^1S) ($n = 2-5$) states (solid lines) and in $1sns$ (^3S) ($n = 2-5$) states (dashed lines) with respect to cavity width Δ (a.u.). Cavity depth V_0 is fixed at 0.5 a.u.

Total Coulomb potential energy v_t^c can further be obtained by putting the value of t and v_{cw} from Eq. (23) and Eq. (20) in Eq. (18). Thus,

$$v_t^c = 2\left(e - V_0\frac{de}{dV_0} + \Delta\frac{de}{d\Delta}\right). \tag{24}$$

Using Eq. (24) and Eq. (21), Coulomb repulsion potential energy (v_{12}^c) can be written as

$$v_{12}^c = 2\left(e - V_0\frac{de}{dV_0} + \Delta\frac{de}{d\Delta}\right) - Z\frac{de}{dZ}. \tag{25}$$

2. $He^+(1s)$ *threshold*

Nonrelativistic Hamiltonian of hydrogen atom under FO potential reads as

$$H = T + V_c + V_{cw}, \tag{26}$$

where $T = -\frac{1}{2}\nabla^2$, $V_c = -\frac{Z}{r}$ and $V_{cw} = -V_0(1 + c_w r)e^{-c_w r}$. By considering $t = \langle T\rangle$, $v_c = \langle V_c\rangle$, and $v_{cw} = \langle V_{cw}\rangle$, we can write the total energy eigenvalue as

$$e = t + v_c + v_{cw}. \tag{27}$$

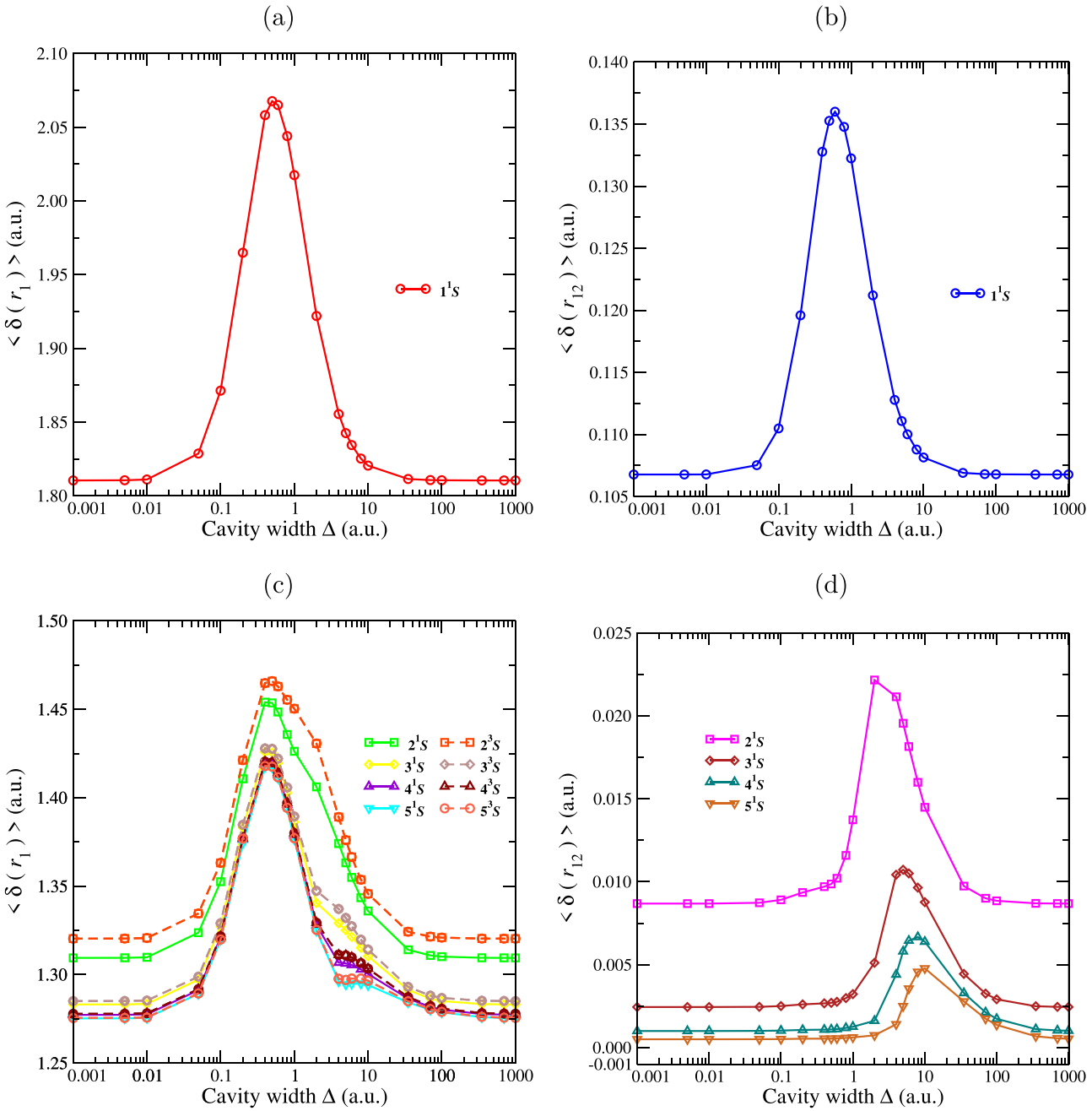

FIG. 9. Variation of the expectation value of (a) one-electron delta function $\delta(\vec{r}_1)$ of He in ground state, (b) two-electron delta function $\delta(\vec{r}_{12})$ of He in ground state, (c) one-electron delta function $\delta(\vec{r}_1)$ of He in $1sns$ (^1S) ($n = 2-5$) states (solid lines) and in $1sns$ (^3S) ($n = 2-5$) states (dashed lines), (d) two-electron delta function $\delta(\vec{r}_{12})$ of He in $1sns$ (^1S) ($n = 2-5$) states (solid lines) and in $1sns$ (^3S) ($n = 2-5$) states (dashed lines), with respect to cavity width Δ. Cavity depth V_0 is fixed at 0.5. All entities are in a.u.

Using Hellmann-Feynman theorem and considering Δ as a parameter, one can write

$$u = \frac{\Delta}{V_0}\frac{de}{d\Delta}, \tag{28}$$

where $u = -c_w^2\langle r^2 e^{-c_w r}\rangle$. Using Eq. (28), the Hellmann-Feynman theorem with respect to V_0 yields

$$v_{cw} = V_0\frac{de}{dV_0} - \frac{\Delta}{2}\frac{de}{d\Delta}. \tag{29}$$

Further using virial theorem, it is straightforward to show that

$$2t + v_c = -\frac{de}{d\Delta}. \tag{30}$$

Now using Eqs. (27), (29), and (30), we find

$$t = V_0\frac{de}{dV_0} - \frac{3}{2}\Delta\frac{de}{d\Delta} - e \tag{31}$$

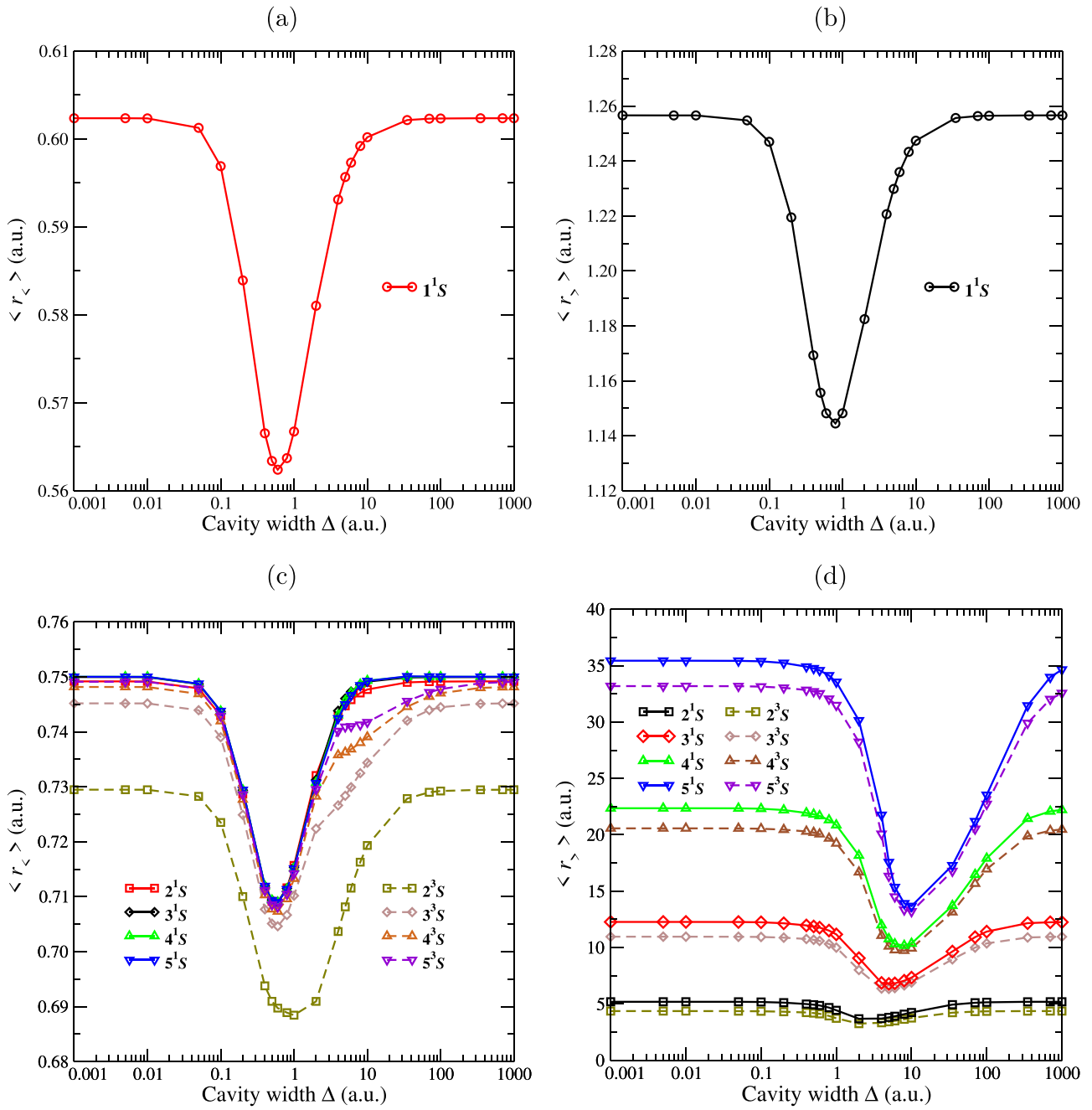

FIG. 10. Variation of the expectation value of (a) inner electron radius $r_<$ of He in ground state, (b) outer electron radius $r_>$ of He in ground state, (c) inner electron radius $r_<$ of He in $1sns$ (^1S) ($n = 2 - 5$) states (solid lines) and in $1sns$ (^3S) ($n = 2 - 5$) states (dashed lines), (d) outer radius $r_>$ of He in $1sns$ (^1S) ($n = 2 - 5$) states (solid lines) and in $1sns$ (^3S)($n = 2 - 5$) states (dashed lines), with respect to cavity width Δ. Cavity depth V_0 is fixed at 0.5. All entities are in a.u.

and thus, from Eq. (27), it can be shown that

$$v_c = 2\left(e - V_0\frac{de}{dV_0} + \Delta\frac{de}{d\Delta}\right). \tag{32}$$

A detailed study on the verification of the Hellmann-Feynman and virial theorem under FO potential has been performed on the ground state of a He atom and the corresponding different energy components which are defined in Eqs. (23), (21), (25), and (20) have been summarized in Table IX. Remarkably, all the energy components estimated from Hellmann-Feynman and virial theorem show good agreement with the data presented in Table II. Specifically, kinetic energy (t) estimated from the Hellmann-Feynman and virial theorem is −3.24585002 a.u. for Δ = 1.0 a.u. and $V_0 = 0.5$ a.u., whereas the value of the same has been reported as −3.24584969 a.u. in Table II. Similarly, the value of v_{12}^c obtained from the Hellmann-Feynman and virial theorem and the same from Table II for $V_0 = 1.0$ a.u. and Δ = 1.0 a.u. yield 1.06067543 a.u. and 1.06067672 a.u., respectively. It has been observed that for any value of Z, de/dZ is always negative and it decreases rapidly as Z increases. Interestingly, de/dZ is also very much sensitive with the strength of the FO potential. It

TABLE IX. Validation test of Hellmann-Feynman and virial theorem corresponding to ($1s^2$, ^1S) state of He and ($1s$, ^2S) state of He^+ for different cavity widths Δ and cavity depths V_0. All entities are in a.u.

		$1s^2$, ^1S				$1s$, ^{2}S		
V_0	Δ	t	$-v_1^c$	v_{12}^c	$-v_{cw}$	t	$-v_c$	$-v_{cw}$
0.5	0.001	2.90372457	6.75326563	0.94581669	0.00000006	2.00000004	4.00000008	0.0
	1.0	3.24585002	7.15945039	1.02286319	0.67416750	2.15667936	4.15302872	0.36721000
	1000.0	2.90372676	6.75326846	0.94581733	0.99999881	1.99999963	3.99999926	0.50000000
1.0	0.001	2.90372545	6.75326760	0.94581777	0.00000036	2.00000025	4.00000050	0.0
	1.0	3.41199947	7.34671771	1.06067543	1.58929880	2.22261445	4.21498390	0.83557250
	1000.0	2.90372676	6.75326945	0.94581832	1.99999881	1.99999963	3.99999926	1.00000000

is noted that for a specific value of V_0, the value of de/dZ decreases for both small and large Δ and in the intermediate region it has a maxima. We have observed an asymptotic nature of the derivative $de/d\Delta$ that becomes zero for both $\Delta \to 0$ and $\Delta \to \infty$. In contrast, for a specific V_0, the derivative term $V_0 de/dV_0 \to 0$ for $\Delta \to 0$ while $V_0 de/dV_0 \to -2V_0$ for $\Delta \to \infty$. We have included the results obtained from virial and the Hellmann-Feynman theorem corresponding to He^+ ($1s$) ion under FO potential and all the energy components which are represented by Eqs. (29), (31), and (32) have been listed in Table IX.

G. Quantum similarity index

The quantum similarity measure between two isolated atoms is defined as [122,123]

$$\mathcal{M}_{AB} \equiv \int \rho_A(\vec{r}_1)\delta(\vec{r}_1 - \vec{r}_2)\rho_B(\vec{r}_2)d\vec{r}_1 d\vec{r}_2, \tag{33}$$

where $\rho_A(\vec{r}_1)$ and $\rho_B(\vec{r}_2)$ are the spinless one-electron radial density for systems A and B, respectively. Now Eq. (33) can be recast as

$$\mathcal{M}_{AB} = 4\pi \int \rho_A(r)\rho_B(r)r^2 dr, \tag{34}$$

where the one-electron radial density $\rho(r_1)$ estimated from the two-electron wave function Ψ is of the form

$$\rho(r_1) = \frac{2\pi}{r_1}\int_0^\infty \int_{|\vec{r}_1-\vec{r}_2|}^{r_1+r_2} |\Psi|^2 r_2 r_{12} dr_2 dr_{12}. \tag{35}$$

Therefore, the QSI can be defined as

$$\mathtt{QSI} = \frac{\mathcal{M}_{AB}}{\sqrt{\mathcal{M}_{AA}\,\mathcal{M}_{BB}}} \tag{36}$$

and quantum dissimilarity between two systems A and B is given by

$$D_{AB} \equiv \mathcal{M}_{AA} + \mathcal{M}_{BB} - 2\mathcal{M}_{AB}. \tag{37}$$

We have investigated four different cases corresponding to QSI based on one-electron radial density normalized to 1 (1-N density) of (i) [He($1s^2$, ^1S); He^+ ($1s$, ^2S)], (ii) [He($1s2s$, ^1S); He^+ ($1s$, ^2S)], (iii) [He($1s2s$, ^3S); He^+ ($1s$, ^2S)], and (iv) [He($1s2s$, ^1S); He($1s2s$, ^3S)] which are summarizedin Table X. It is to be noted that for constant cavity depth V_0, the similarity between He($1s^2$, ^1S) and He^+ ($1s$, ^2S) increases up to a certain value of Δ and then it again decreases with the increment of Δ. In contrast, quantum dissimilarity (D_{AB}) between the two systems He ($1s^2$, ^1S) and He^+ ($1s$, ^2S) decreases initially up to a specific value of Δ beyond which dissimilarity increases. We have identified that the increment of V_0 increases the similarity and decreases the dissimilarity value. To demonstrate the exactness of the results, we have listed the value of normalization constants N_1 and N_2 in the third and fourth columns of Table X corresponding to systems A and B, respectively. The variation of QSI between He ($1s^2$, ^1S) and He^+ ($1s$, ^2S) for $V_0 = 0.5$ a.u. with respect to Δ is clearly depicted in Fig. 11(a). Interestingly, a sharp peak of the QSI at around $\Delta = 1.0$ a.u. can be visualized from the figure. Moreover, variation of QSI is very prominent within the region $\Delta = 0.1 - 10.0$ a.u. and, beyond that region, the value of the QSI is almost constant with value 0.99446. It is observed that unlike the QSI between the He ($1s^2$, ^1S) and He^+ ($1s$, ^2S), in this case QSI decreases initially up to a Δ value and then it increases again. In addition, the value of QSI always remains higher for the set [He^+ ($1s$, ^2S); He ($1s2s$, ^1S)] as compared to [He^+ ($1s$, ^2S); He ($1s2s$, ^3S)] for any arbitrary value of V_0 and Δ. Specifically, the QSI of the set [He^+ ($1s$, ^2S); He ($1s2s$, ^1S)] for $\Delta = 1.0$ a.u., and $V_0 = 0.5$ a.u. is 0.99874275

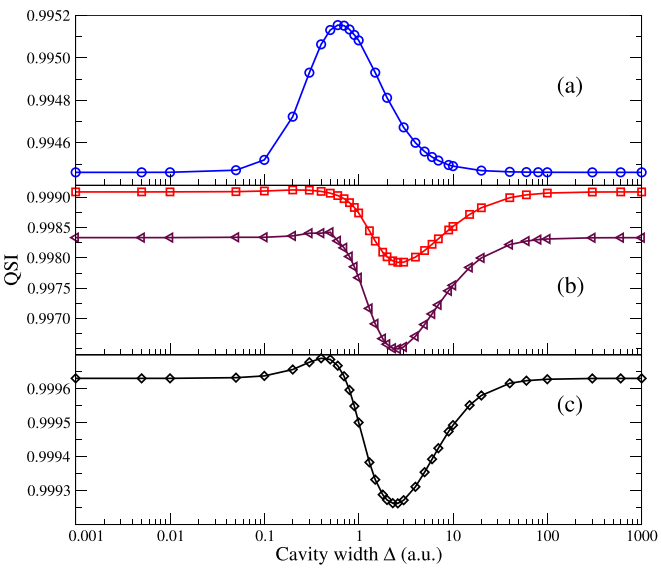

FIG. 11. Variation of quantum similarity index (QSI) between (a) He ($1s^2$, ^1S) and He^+ ($1s$, ^2S) (○, blue line), (b) He ($1s2s$, ^1S) and He^+($1s$, ^2S) (□, red line), He ($1s2s$, ^3S) and He^+ ($1s$, ^2S) (◁, maroon line), (c) He ($1s2s$, ^1S) and He ($1s2s$, ^3S) (◇, black line) with respect to cavity width Δ (a.u.). Cavity depth V_0 is fixed at 0.5 a.u.

TABLE X. Quantum similarity measures $\mathcal{M}_{AB}$, $\mathcal{M}_{AA}$, and $\mathcal{M}_{BB}$, quantum similarity index (QSI) and quantum dissimilarity D_{AB} between systems A and B for different cavity widths Δ and cavity depths V_0. N_1 and N_2 represent the normalization constant corresponding to systems A and B, respectively. All entities are in a.u.

V_0	Δ	N_1	N_2	$\mathcal{M}_{AB}$	$\mathcal{M}_{AA}$	$\mathcal{M}_{BB}$	QSI	D_{AB}
		A: He^+ ($1s$, ^2S), B: He ($1s^2$, ^1S)						
0.5	0.001	0.99999964	0.99999996	0.24524715	0.43711054	0.56418951	0.99446083	0.01888113
	1.0	0.99999974	0.99999997	0.28448389	0.47681990	0.59957575	0.99508287	0.01788051
	100.0	0.99999962	0.99999997	0.24526922	0.43713783	0.56420486	0.99446117	0.01887817
1.0	0.001	0.99999964	0.99999997	0.24524725	0.56418962	0.43711063	0.99446083	0.01888114
	1.0	0.99999974	0.99999997	0.30100373	0.61054046	0.49531855	0.99534315	0.01609266
	100.0	0.99999965	0.99999997	0.24526295	0.56418964	0.43713801	0.99446218	0.01887369
		A: He^+ ($1s$, ^{2}S), B: He ($1s2s$, ^1S)						
0.5	0.001	0.99999936	0.99999756	0.16428488	0.56418885	0.29145288	0.99909031	0.07468407
	1.0	0.99999938	0.99999975	0.18562003	0.31124312	0.59713350	0.99874275	0.08220064
	100.0	0.99999931	0.99999845	0.16438622	0.29163040	0.56420420	0.99907089	0.07460222
1.0	0.001	0.99999934	0.99999659	0.16429477	0.56418897	0.29147045	0.99909004	0.07467466
	1.0	0.99999938	0.99999980	0.20194981	0.61053971	0.33161395	0.99746290	0.07882692
	100.0	0.99999936	0.99999817	0.16439558	0.56418898	0.29165508	0.99907013	0.07458074
		A: He^+ ($1s$, ^{2}S), B: He ($1s2s$, ^3S)						
0.5	0.001	0.99999936	0.99999960	0.16399822	0.56418885	0.29116435	0.99833532	0.07508930
	1.0	0.99999938	0.99999980	0.18619253	0.31253723	0.59713350	0.99767490	0.08186289
	100.0	0.99999931	0.99999969	0.16406151	0.29127525	0.56420420	0.99831320	0.07504463
1.0	0.001	0.99999934	0.99999957	0.16399889	0.56418896	0.29116549	0.99833529	0.07508875
	1.0	0.99999938	0.99999979	0.20227646	0.61053971	0.33274705	0.99567412	0.07892640
	100.0	0.99999936	0.99999969	0.16405873	0.56418898	0.29127832	0.99831265	0.07503481
		A: He ($1s2s$, ^1S), B: He ($1s2s$, ^3S)						
0.5	0.001	0.99999960	0.99999756	0.08482937	0.29145288	0.29116435	0.99963094	0.00006272
	1.0	0.99999980	0.99999975	0.09722652	0.31124312	0.31253723	0.99950101	0.00009875
	100.0	0.99999960	0.99999757	0.08483030	0.29145489	0.29116554	0.99963091	0.00006273
1.0	0.001	0.99999957	0.99999659	0.08483481	0.29116549	0.29147045	0.99963091	0.00006274
	1.0	0.99999979	0.99999979	0.11025129	0.33274705	0.33161395	0.99916372	0.00018584
	100.0	0.99999969	0.99999817	0.08492126	0.29127832	0.29165508	0.99962868	0.00006323

as compared to the value 0.99767490 corresponding to the set [He^+ ($1s$, ^2S); He ($1s2s$, ^3S)] with same Δ and V_0. To visualize this, we have plotted the variation of the QSI between He^+($1s$, ^2S) and He($1s$, $^{1,3}S$) as a function of Δ for $V_0 = 0.5$ a.u., which is shown in Fig. 11(b). Red solid line with square symbol represents the QSI between He^+($1s$, ^2S) and He ($1s$, ^1S) while the QSI between He^+ ($1s$, ^2S) and He ($1s$, ^3S) is shown by maroon solid line with triangle symbol. Table X also contains the results of the same systems corresponding to $V_0 = 1.0$ a.u. It can be noted that the value QSI between He ($1s2s$, ^1S) and He ($1s2s$, ^3S) for any V_0 and Δ is very close to unity, which is evidently due to the strong similarity between the electron probability density distribution of the two systems. Smaller values of the quantum dissimilarity (D_{AB}) that are listed in the last column of Table X strengthens this fact further. In Fig. 11(c) (black line), QSI between He ($1s2s$, ^1S) and He ($1s2s$, ^3S) has been presented for different values of Δ and $V_0 = 0.5$ a.u. It is noted that QSI between the singlet and triplet He ($1s2s$) state has a minimum value within a range $\Delta = 0.5$ to 100.0 a.u. and outside of which it has a constant value 0.99963.

H. Shannon information entropy

The Shannon information entropy [124] of an atomic system is a measure of the spread or the extent of delocalization of the total electronic charge density. The more the delocalization in the electron radial charge distribution, the larger the Shannon information entropy of the system. In a nutshell, Shannon information entropy measures the probability distribution of a system and it is associated with statistical correlation between the particles of a system. While the von Neumann entropy and linear entropy (linear approximation of von Neumann entropy) are the measures of quantum correlations between the particles, the details of which have been discussed in Sec. III D. The Shannon information entropy (S) in position space for case of a multielectron system can be defined by the one-electron radial density $\rho(r)$ as follows [19]:

$$S = -\int_0^\infty \rho(r) \ln \rho(r) 4\pi r^2 dr. \tag{38}$$

The one-electron radial density $\rho(r_1)$ for the case of a He atom is given by Eq. (35) and is taken to be 1-normalized.

TABLE XI. Comparison of present Shannon information entropy S of ($1s^2$, ^1S) and ($1s2s$, $^{1,3}S$) states of He with available theoretical calculations for different cavity widths Δ and cavity depths V_0. All entities are in a.u. *a*, *b*: Ou and Ho [19,74], *c*: Lin and Ho [88], *d*: Restrepo Cuartas and Sanz-Vicario [89].

		$1s^2$, ^1S		$1s2s$, ^1S		$1s2s$, ^3S	
V_0	Δ	Present	Others	Present	Others	Present	Others
Free	–	2.70509	2.70510285[a]	5.49136	5.49196837[a]	5.23596	
			2.70510285[b]		5.49196878[b]		5.23597814[b]
			2.7051028[c]				
			2.705[d]		5.492[d]		5.236[d]
0.5	0.001	2.70509		5.49182		5.23597	
	0.01	2.70503	2.7050463[a]	5.49178		5.23593	
	1.0	2.46613	2.4661404[a]	5.17319	5.1733749[a]	4.89762	
	4.0	2.63293030	2.6329358[a]	4.86851	4.8685244[a]	4.718830	
	100.0	2.70486	2.7048699[a]	5.47552	5.4755194[a]	5.22589	
	1000.0	2.70509		5.49164		5.23586	
1.0	0.001	2.70509		5.49182		5.23597	
	1.0	2.34930		4.57870		4.37750	
	1000.0	2.70509		5.49164		5.23586	

In Table XI, we have made a comparative study on some of our computed results corresponding to He ($1s^2$, ^1S) and He ($1s2s$, $^{1,3}S$) for free as well as for different values of Δ and V_0 by considering $N = 34$ terms in the wave function. It is evident from Table XI that the results presented in this paper are in good agreement with the work done by different researchers [19,74,88,89]. Figure 12 depicts the detailed variation of Shannon entropy of the ground state of He atom with $V_0 = 0.5$ a.u. and for different values of Δ. Over the range of small values of Δ in Fig. 12, designated by points *A* and *B*, as well as over the range of large values of Δ (points *D* and *E*), the FO potential is not effectively felt by the electrons. It becomes relevant over the intermediate range marked by *B*–*D*. An increase in the width at the end of the narrow range of values of Δ (point *B*) where the FO potential starts to become relevant, leads to an increase in the localization of the charge density which is reminiscent of the increase in the nuclear charge along the isoelectronic series. Similar localization effect is observed at the other end as Δ decreases over the range marked by points *D* and *C*. There exists a characteristic width at a given fixed depth of the FO potential corresponding to which the Shannon information entropy is at its minimum value (maximum charge localization). We recall here that the variation of the electron repulsion terms in Sec. III B, Fig. 3 has been rationalized earlier in the similar manner.

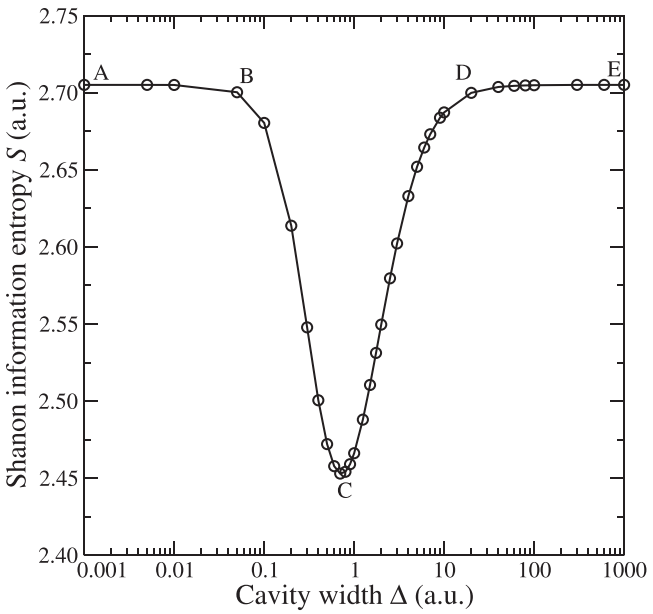

FIG. 12. Variation of Shannon information entropy S of the ground state of He with respect to cavity width Δ. Cavity depth V_0 is fixed at 0.5. All entities are in a.u.

IV. CONCLUSION

Precise structural properties, quantum similarity, entanglement, and information theoretic measures corresponding to the $1sns$ ($^{1,3}S$) ($n = 1 - 5$) states of He atoms under the influence of two-parameter FO model potential mimicking a QD environment have been estimated in the framework of Ritz variational method and explicitly correlated multiexponent Hylleraas-type basis set. A detailed analysis of the results has been presented, which reveals several characteristic features of the embedded He atom. The main findings are listed as follows:

(1) We have noted that the increment of any single parameter (cavity width Δ or cavity depth V_0) in the FO potential changes the overall physical characteristics of the He atom. However, it is observed that for a constant potential depth V_0, the structural changes of $1sns$ ($^{1,3}S$) ($n = 1 - 5$) states of a He atom under the FO potential are the most prominent over the approximate range of cavity width $\Delta = 0.1$ to 10 a.u. for a fixed depth V_0.

(2) We have verified the Hund's spin multiplicity rule for $1sns$ ($^{1,3}S$) ($n = 2 - 5$) states of He atom. For a fixed V_0, as Δ increases, the electron repulsion energy of the triplet S states is found to be larger than the singlet S states when Δ is either too

small or too large. At the intermediate range of Δ values, this trend is reversed. The difference between the repulsion energy of singlet and triplet statesdecreases with the increment of the n value.

(3) It has been observed that the energy contribution from radial and angular correlation changes with the increasing influence of the FO potential. For a constant V_0 and small Δ, the major contribution of the correlation energy comes from the angular correlation limit, which increases up to a certain value of Δ. In contrast, the energy contribution from the radial correlation limit is less and it decreases further with the increment of Δ.

(4) It is observed that an arbitrary increase in the strength of the FO potential cannot ionize the He atom or, in other words, the ground state of He atom stays lower than that of the respective first ionization threshold throughout the entire range of cavity width.

(5) The expectation value of different radial quantities r_1, r_1^2, r_{12}, r_{12}^2, $r_<$, $r_>$, angular quantities θ_1, θ_{12}, one-particle delta function $\delta(\vec{r}_1)$ and two-particle delta function $\delta(\vec{r}_{12})$ have been estimated with high precision and depicted some unique variations.

(6) The different energy components both for the ground states of confined He atom and its respective first ionization threshold estimated with aid the Hellmann-Feynman theorem and the virial theorem are found to be in quantitative agreement with their values calculated from direct variationally optimized wave functions. Such an agreement between the two sets of values establish the high quality of the calculations reported in this paper.

(7) The nonmonotonic nature of QSI and dissimilarity (D) estimated electron charge distribution among ($1s$, ^2S) state of He^+ ions and ($1sns$, $^{1,3}S$) states ($n = 1, 2$) of He atoms have been observed and it is found that the QSI as well as D undergoes a sharp changes within the approximate range of cavity width $\Delta = 0.1$ to 10 a.u.

(8) Within the aforementioned range, the von Neumann entropy, linear entropy, and Shannon entropy experience the maximum effect of FO potential and, beyond that range, the value of the same almost remains constant.

It is hoped that the present paper involving the FO potential will stimulate more investigations involving different, other model-confining potentials, which would give rise to interesting changes in the properties of He atoms.

ACKNOWLEDGMENTS

J.K.S. acknowledges partial financial support from the Department of Science and Technology, Govt. of West Bengal under Grant No. 249(Sanc.)/ST/P/S&T16G-26/2017. K.D.S. acknowledges the financial support from the Indian National Science Academy, New Delhi under the Grant No. INSA/SP/SS/2021/MAY21. K.D.S. thanks Shiro L. Saito for a copy of the HF code and gratefully acknowledges fruitful discussions with Jacob Katriel on the Hund's rule section of the present paper. The authors are thankful to anonymous referees for making useful suggestions which led to substantial improvement in the presentation of this paper.

[1] N. A. of Sciences Engineering and Medicine, *Manipulating Quantum Systems: An Assessment of Atomic, Molecular, and Optical Physics in the United States* (The National Academies Press, Washington, DC, 2020).
[2] C. Y. Lin and Y. K. Ho, Phys. Rev. A **84**, 023407 (2011).
[3] J. A. Ludlow, T. G. Lee, and M. S. Pindzola, J. Phys. B: At. Mol. Opt. Phys. **43**, 235202 (2010).
[4] L. Türker, Int. J. Hydrogen Energy **32**, 1933 (2007).
[5] J. K. Saha, S. Bhattacharyya, and T. K. Mukherjee, Phys. Plasmas **23**, 092704 (2016).
[6] D. J. Norris, A. L. Efros, and S. C. Erwin, Science **319**, 1776 (2008).
[7] N. L. Rosi, J. Eckert, M. Eddaoudi, D. T. Vodak, J. Kim, M. O'Keeffe, and O. M. Yaghi, Science **300**, 1127 (2003).
[8] *Solvation Effects on Molecules and Biomolecules*, Challenges and Advances in Computational Chemistry and Physics, edited by S. Canuto (Springer, Dordrecht, 2010).
[9] A. Sil, S. Canuto, and P. Mukherjee, Spectroscopy of Confined Atomic Systems: Effect of Plasma, *Advances in Quantum Chemistry*, Vol. 58 (Academic Press, 2009), pp. 115–175.
[10] W. Jaskólski, Phys. Rep. **271**, 1 (1996).
[11] A. P. Alivisatos, Science **271**, 933 (1996).
[12] *The Theory of Confined Quantum Systems, Parts I and II*, Advances in Quantum Chemistry, edited by J. Sabin, E. Brandas, and S. Cruz (Academic Press, 2009), Vol. 57.
[13] *Electronic Structure of Quantum Confined Atoms and Molecules*, edited by K. D. Sen (Springer, Cham, 2014).
[14] E. Ley Koo, Rev. Mex. Física **64**, 326 (2018).
[15] V. AquilantiH. E. Montgomery, C. N. Ramachandran, and N. Sathyamurthy, Eur. Phys. J. D **75**, 187 (2021).
[16] G. Schedelbeck, W. Wegscheider, M. Bichler, and G. Abstreiter, Science (NY) **278**, 1792 (1997).
[17] X. Michalet, F. F. Pinaud, L. A. Bentolila, J. M. Tsay, S. Doose, J. J. Li, G. Sundaresan, A. M. Wu, S. S. Gambhir, and S. Weiss, Science (NY) **307**, 538 (2005).
[18] Y. C. Cao, Science **332**, 48 (2011).
[19] J. H. Ou and Y. K. Ho, Atoms **5**, 15 (2017).
[20] A. Franciosi and C. G. Van de Walle, Surf. Sci. Rep. **25**, 1 (1996).
[21] T. V. Bezyazychnaya, M. V. Bogdanovich, V. V. Kabanov, D. M. Kabanau, Y. V. Lebiadok, V. V. Parashchuk, A. G. Ryabtsev, G. I. Ryabtsev, P. V. Shpak, M. A. Shchemelev, I. A. Andreev, E. V. Kunitsyna, V. V. Sherstnev, and Y. P. Yakovlev, Semiconductors **49**, 980 (2015).
[22] C. Belver, J. Bedia, and J. Rodriguez, Appl. Catal., B **176–177**, 278 (2015).
[23] E. Kasapoglu, H. Sari, and I. Sökmen, Phys. B: Condens. Matter **353**, 345 (2004).
[24] R. K. Pandey, M. K. Harbola, and V. A. Singh, J. Phys.: Condens. Matter **16**, 1769 (2004).

[25] C. M. Lee, C. C. Lam, and S. W. Gu, Phys. Rev. B **61**, 10376 (2000).
[26] M. Genkin and E. Lindroth, Phys. Rev. B **81**, 125315 (2010).
[27] R. J. Yánez, W. Van Assche, and J. S. Dehesa, Phys. Rev. A **50**, 3065 (1994).
[28] S. R. Gadre, Phys. Rev. A **30**, 620 (1984).
[29] P. Winkler, Int. J. Quantum Chem. **100**, 1122 (2004).
[30] J. K. Saha, S. Bhattacharyya, and T. Mukherjee, Commun. Theor. Phys. **65**, 347 (2016).
[31] P. Kimani, P. Jones, and P. Winkler, Int. J. Quantum Chem. **108**, 2763 (2008).
[32] S. Chakraborty and Y. K. Ho, Phys. Rev. A **84**, 032515 (2011).
[33] M. C. Onyeaju, J. O. A. Idiodi, A. N. Ikot, M. Solaimani, and H. Hassanabadi, Few-Body Syst. **57**, 793 (2016).
[34] M. Şahin, J. Appl. Phys. **106**, 063710 (2009).
[35] L. Juharyan, E. Kazaryan, and L. Petrosyan, Solid State Commun. **139**, 537 (2006).
[36] Z. Parang, A. Keshavarz, and N. Zamani, J. Comput. Electron. **13**, 1020 (2014).
[37] R. Khordad and B. Mirhosseini, Opt. Spectrosc. **117**, 434 (2014).
[38] R. Khordad and B. Mirhosseini, Pramana - J. Phys. **85**, 723 (2015).
[39] L. G. Jiao and Y. K. Ho, in *Quantum Confined Electronic Structure of Atoms and Molecules*, edited by K. D. Sen (Springer, Cham, 2014).
[40] N. M. Cann, R. J. Boyd, and A. J. Thakkar, Int. J. Quantum Chem. **48**, 33 (1993).
[41] A. M. Frolov, J. Chem. Phys. **126**, 104302 (2007).
[42] L. G. Jiao, L. R. Zan, L. Zhu, and Y. K. Ho, Comput. Theor. Chem. **1135**, 1 (2018).
[43] M. A. Nielsen and I. L. Chuang, *Quantum Computation and Quantum Information* (Cambridge University Press, Cambridge, UK, 2010).
[44] M. C. Tichy, F. Mintert, and A. Buchleitner, J. Phys. B: At., Mol. Opt. Phys. **44**, 192001 (2011).
[45] S. Abdullah, J. P. Coe, and I. D'Amico, Phys. Rev. B **80**, 235302 (2009).
[46] L. Amico, R. Fazio, A. Osterloh, and V. Vedral, Rev. Mod. Phys. **80**, 517 (2008).
[47] A. Kuroś and A. Okopińska, in *Quantum Systems in Physics, Chemistry and Biology - Theory, Interpretation, and Results*, Advances in Quantum Chemistry, edited by S. Jenkins, S. R. Kirk, J. Maruani, and E. J. Brändas (Academic Press, 2019), Vol. 78, pp. 31–55.
[48] J. S. Dehesa, T. Koga, R. J. Y.áñez, A. R. Plastino, and R. O. Esquivel, J. Phys. B: At., Mol. Opt. Phys. **45**, 015504 (2012).
[49] J. S. Dehesa, T. Koga, R. J. Yáñez, A. R. Plastino, and R. O. Esquivel, J. Phys. B: At., Mol. Opt. Phys. **45**, 239501 (2012).
[50] G. Benenti, S. Siccardi, and G. Strini, Eur. Phys. J. D **67**, 83 (2013).
[51] Y. C. Lin, C. Y. Lin, and Y. K. Ho, Phys. Rev. A **87**, 022316 (2013).
[52] C. H. Lin, Y. C. Lin, and Y. K. Ho, Few-Body Syst. **54**, 2147 (2013).
[53] T. Hofer, Front. Chem. **1**, 24 (2013).
[54] P. Kościk and A. Okopińska, Few-Body Syst. **55**, 1151 (2014).
[55] C.-H. Lin and Y. K. Ho, Few-Body Syst. **55**, 1141 (2014).
[56] C.-H. Lin and Y. K. Ho, Few-Body Syst. **56**, 157 (2015).
[57] R. O. Esquivel, S. López-Rosa, and J. S. Dehesa, Europhys. Lett. **111**, 40009 (2015).
[58] Y. K. Ho and C.-H. Lin, J. Phys.: Conf. Ser. **635**, 092025 (2015).
[59] Y. K. Ho, JPS Conf. Proc. **18**, 011027 (2017).
[60] Y. C. Lin and Y. K. Ho, Can. J. Phys. **93**, 646 (2015).
[61] Y. C. Lin, T. K. Fang, and Y. K. Ho, Phys. Plasmas **22**, 032113 (2015).
[62] H. T. Peng and Y. K. Ho, Mod. Phys. Lett. B **29**, 1550189 (2015).
[63] J. Wang, C. K. Law, and M. C. Chu, Phys. Rev. A **72**, 022346 (2005).
[64] B. Sun, D. L. Zhou, and L. You, Phys. Rev. A **73**, 012336 (2006).
[65] L. He and A. Zunger, Phys. Rev. B **75**, 075330 (2007).
[66] J. P. Coe, A. Sudbery, and I. D'Amico, Phys. Rev. B **77**, 205122 (2008).
[67] O. Osenda and P. Serra, Phys. Rev. A **75**, 042331 (2007).
[68] P. Kościk, Few-Body Syst. **52**, 49 (2012).
[69] D. S. A. Coden, R. H. Romero, A. Ferrón, and S. S. Gomez, J. Phys. B: At., Mol. Opt. Phys. **46**, 065501 (2013).
[70] P. Kościk, Phys. Lett. A **377**, 2393 (2013).
[71] P. Kościk and J. K. Saha, Few-Body Syst. **56**, 645 (2015).
[72] J. Szabo, K. Sen, and A. Nagy, Phys. Lett. A **372**, 2428 (2008).
[73] E. Romera and J. S. Dehesa, J. Chem. Phys. **120**, 8906 (2004).
[74] J.-H. Ou and Y. K. Ho, Atoms **7**, 70 (2019).
[75] N. L. Guevara, R. P. Sagar, and R. O. Esquivel, Phys. Rev. A **67**, 012507 (2003).
[76] J.-H. Ou and Y. K. Ho, Int. J. Quantum Chem. **119**, e25928 (2019).
[77] K. D. Sen, ed., *Statistical complexity* (Springer, Dordrecht, 2011).
[78] J. C. Angulo and S. López-Rosa, Entropy **24**, 233 (2022).
[79] R. P. Sagar and N. L. Guevara, J. Chem. Phys. **123**, 044108 (2005).
[80] R. P. Sagar, H. G. Laguna, and N. L. Guevara, Chem. Phys. Lett. **514**, 352 (2011).
[81] S. López-Rosa, A. L. Martín, J. Antolín, and J. C. Angulo, Int. J. Quantum Chem. **119**, e25861 (2019).
[82] R. P. Sagar, H. G. Laguna, and N. L. Guevara, Int. J. Quantum Chem. **111**, 3497 (2011).
[83] S. López-Rosa, J. C. Angulo, A. L. Martín, and J. Antolín, Eur. Phys. J. Plus **136**, 763 (2021).
[84] I. Nasser, M. Zeama, and A. Abdel-Hady, Phys. Scr. **95**, 095401 (2020).
[85] C. Martínez-Flores, M. Zeama, and I. Nasser, Phys. Scr. **96**, 065404 (2021).
[86] I. Nasser, C. Martinez-Flores, M. Zeama, R. Vargas, and J. Garza, Phys. Lett. A **392**, 127136 (2021).
[87] I. Nasser, M. Zeama, and A. Abdel-Hady, Int. J. Quantum Chem. **121**, e26499 (2021).
[88] C.-H. Lin and Y. K. Ho, Chem. Phys. Lett. **633**, 261 (2015).
[89] J. P. Restrepo Cuartas and J. L. Sanz-Vicario, Phys. Rev. A **91**, 052301 (2015).
[90] R. P. Sagar, H. G. Laguna, and N. L. Guevara, Mol. Phys. **107**, 2071 (2009).
[91] K. D. Sen, J. Chem. Phys. **123**, 074110 (2005).
[92] J. A. Nelder and R. Mead, Comput. J. **7**, 308 (1965).
[93] C. C. J. Roothaan, Rev. Mod. Phys. **23**, 69 (1951).
[94] C. Roothaan, Rev. Mod. Phys. **32**, 179 (1960).

[95] C. Roothaan and P. Bagus, in *Methods in Computational Physics*, edited by S. F. B. Alder and M. Rotenberg (Academic Press, New York, 1963), Vol. II, p. 47.
[96] S. L. Saito, Theor. Chem. Acc. **109**, 326 (2003).
[97] S. L. Saito, At. Data Nucl. Data Tables **95**, 836 (2009).
[98] S. L. Saito, J. Chem. Phys. **130**, 074306 (2009).
[99] C. d. Boor, *A Practical Guide to Splines*, Applied Mathematical Sciences (Springer, New York, 1978).
[100] T. L. Gilbert and P. J. Bertoncini, J. Chem. Phys. **61**, 3026 (1974).
[101] G. Drake and Z.-C. Van, Chem. Phys. Lett. **229**, 486 (1994).
[102] F. Hund, Z. Phys. **33**, 345 (1925).
[103] F. Hund, Z. Phys. **33**, 855 (1925).
[104] F. Hund, Z. Phys. **34**, 296 (1925).
[105] F. Hund, *Linienspektren und Periodisches System der Elemente* (Springer, Vienna, Austria, 1927).
[106] J. C. Slater, Phys. Rev. **34**, 1293 (1929).
[107] E. R. Davidson, J. Chem. Phys. **42**, 4199 (1965).
[108] J. Katriel, Theor. Chim. Acta **23**, 309 (1972).
[109] J. Katriel, Theor. Chim. Acta **26**, 163 (1972).
[110] J. Katriel and R. Pauncz (Academic Press, 1977), p. 143.
[111] T. Koga and Y. Koshida, J. Chem. Phys. **111**, 54 (1999).
[112] K. Hongo, R. Maezono, Y. Kawazoe, H. Yasuhara, M. D. Towler, and R. J. Needs, J. Chem. Phys. **121**, 7144 (2004).
[113] A. Sarsa, E. Buendía, F. Gálvez, and J. Katriel, Chem. Phys. Lett. **702**, 106 (2018).
[114] J. Katriel, H. E. Montgomery Jr., and K. D. Sen, Phys. Plasmas **25**, 092111 (2018).
[115] J. Katriel, H. E. Montgomery, J. A. Sarsa, E. Buendía, F. J. Gálvez, and K. D. Sen, Nanosystems: Phys. Chem. Math. **10**, 31 (2019).
[116] E. R. Davidson, J. Chem. Phys. **39**, 875 (1963).
[117] E. R. Davidson, Rev. Mod. Phys. **44**, 451 (1972).
[118] T. Koga, J. Chem. Phys. **121**, 3939 (2004).
[119] L. G. Jiao, L. R. Zan, L. Zhu, Y. Z. Zhang, and Y. K. Ho, Phys. Rev. A **100**, 022509 (2019).
[120] G. W. Kellner, Z. Phys. **44**, 0044 (1927).
[121] C. Eckart, Phys. Rev. **35**, 1303 (1930).
[122] R. Carbó, L. Leyda, and M. Arnau, Int. J. Quantum Chem. **17**, 1185 (1980).
[123] P. Bouvrie, J. Antolín, and J. Angulo, Chem. Phys. Lett. **506**, 326 (2011).
[124] C. E. Shannon, Bell Syst. Tech. J. **27**, 379 (1948).